nature metabolism

ARTICLES

https://doi.org/10.1038/s42255-021-00466-9

Check for updates

Fasting drives the metabolic, molecular and geroprotective effects of a calorie-restricted diet in mice

Heidi H. Pak[1,2,3], Spencer A. Haws[3,4,5], Cara L. Green[1,2], Mikaela Koller[1,2], Mitchell T. Lavarias[3,6], Nicole E. Richardson[1,2,7], Shany E. Yang[1,2], Sabrina N. Dumas[1,2], Michelle Sonsalla[1,2], Lindsey Bray[1,2], Michelle Johnson[8], Stephen Barnes[9], Victor Darley-Usmar[8], Jianhua Zhang[8], Chi-Liang Eric Yen[3,6], John M. Denu[3,4,5] and Dudley W. Lamming[1,2,3,7] ✉

Calorie restriction (CR) promotes healthy ageing in diverse species. Recently, it has been shown that fasting for a portion of each day has metabolic benefits and promotes lifespan. These findings complicate the interpretation of rodent CR studies, in which animals typically eat only once per day and rapidly consume their food, which collaterally imposes fasting. Here we show that a prolonged fast is necessary for key metabolic, molecular and geroprotective effects of a CR diet. Using a series of feeding regimens, we dissect the effects of calories and fasting, and proceed to demonstrate that fasting alone recapitulates many of the physiological and molecular effects of CR. Our results shed new light on how both when and how much we eat regulate metabolic health and longevity, and demonstrate that daily prolonged fasting, and not solely reduced caloric intake, is likely responsible for the metabolic and geroprotective benefits of a CR diet.

CR is the gold standard for geroprotective interventions, extending lifespan and health span in diverse organisms and preventing or delaying many age-associated diseases[1–6]. In rodents, CR improves metabolic health and glucose homeostasis[1,7]. As long-term adherence to a reduced-calorie diet is difficult for many people, there is substantial interest in identifying the physiological and molecular mechanisms that mediate the beneficial effects of a CR diet.

Traditionally, the beneficial effects of a CR diet were believed to be the result of reduced caloric intake, although recent studies suggest that reduction of specific macronutrients may also play a role[8–14]. It has recently been realized that CR regimens, as typically implemented in the laboratory, not only restrict calories, but also impose a prolonged daily fast, as CR animals rapidly consume their entire daily meal within ~2 h, and then fast for ~22 h until their next meal[15–17]. Interventions such as time-restricted or meal feeding that involve a fasting period have metabolic benefits and extend the lifespan of mice[18–20]. These findings complicate the interpretation of CR studies, as it is unclear which effects of CR result from reduced caloric intake, and which instead are attributable to the collaterally imposed fast.

We developed a series of diets and feeding regimens enabling us to dissect the contribution of fasting from energy restriction alone in a CR diet. As mice of different strains and sexes have differential responses to a CR diet[21,22], we examined the metabolic responses of both male and female C57BL/6J and DBA/2J mice. We also tested whether prolonged daily fasting without energy restriction could recapitulate the metabolic and transcriptional effects of a CR diet. Finally, we tested if fasting is required for the beneficial effects of a CR diet on health span and longevity.

We find that fasting is required for CR-induced changes in insulin sensitivity and fuel selection. Additionally, fasting alone without reduced energy intake is sufficient to recapitulate the metabolic phenotypes and transcriptional signature of a CR diet. Finally, we show that fasting is required for CR-induced improvements in glucose metabolism, frailty and lifespan in C57BL/6J male mice. Our results overturn the long-held belief that the beneficial effects of a CR diet in mammals are mediated solely by the reduction of caloric intake, and highlight fasting as an important component of the metabolic and geroprotective effects of CR.

Results

The response of C57BL/6J males to multiple feeding paradigms. We acclimatized 9-week-old C57BL/6J male (B6M) mice for 1 week to a chow-based diet (Envigo Global 2018)[21]. The animals were then weighed and randomized to one of four dietary regimens (Fig. 1a):

1. AL, mice given ad libitum access to a normal rodent diet (Envigo Global 2018; Supplementary Table 1).
2. Diluted AL, mice provided with ad libitum access to Envigo Global 2018 diluted 50% with indigestible cellulose (TD.170950; Supplementary Table 1); equivalent to 30% restriction of calories without imposed fasting[8].

[1]Department of Medicine, University of Wisconsin–Madison, Madison, WI, USA. [2]William S. Middleton Memorial Veterans Hospital, Madison, WI, USA. [3]Interdisciplinary Graduate Program in Nutritional Sciences, University of Wisconsin–Madison, Madison, WI, USA. [4]Department of Biomolecular Chemistry, University of Wisconsin–Madison, Madison, WI, USA. [5]Wisconsin Institute for Discovery, Madison, WI, USA. [6]Department of Nutritional Sciences, University of Wisconsin–Madison, Madison, WI, USA. [7]Endocrinology and Reproductive Physiology Graduate Training Program, University of Wisconsin–Madison, Madison, WI, USA. [8]Nathan Shock Center of Excellence in the Basic Biology of Aging, Department of Pathology, University of Alabama, Birmingham, Birmingham, AL, USA. [9]Department of Pharmacology, University of Alabama, Birmingham, Birmingham, AL, USA. ✉e-mail: dlamming@medicine.wisc.edu

3. MF.cr, mice were fed 30% less food than AL-fed mice, using an automatic feeder to release food in three equal portions during the 12-h dark period; meal feeding (MF) reduces fasting period and binging behaviour.
4. CR, mice fed once per day in the morning; with 30% restriction relative to the AL group and prolonged inter-meal fasting.

The feeding times for the CR and MF.cr diets were carefully considered. Feeding CR mice once per day in the morning has been widely utilized for CR studies, including by the National Institute on Aging (NIA) aged rodent colony[23], and is well established to extend lifespan. Furthermore, the time of day at which the feeding of CR mice occurs does not affect the ability of CR to extend lifespan[24]. Feeding MF.cr mice overnight during the dark cycle aligns the completion-of-feeding time of the CR and MF.cr groups, and this MF.cr regimen is similar to a regimen previously shown to extend the lifespan of mice[24].

Some of the most well-established effects of a CR diet include reduced weight gain and adiposity[7,25,26]. Tracking the mice on each diet regimen, we found that all three dietary restriction regimens reduced weight gain, fat mass and adiposity (Fig. 1b–e and Supplementary Table 2a). Despite all three diets reducing calorie intake by 30% (Extended Data Fig. 1a), there were clear differences between the effects of the diets. CR-fed mice gained more weight than mice fed the Diluted AL diet or the MF.cr diet (Fig. 1b and Supplementary Table 2a). Additionally, all three groups initially lost lean (fat-free) mass to differing degrees, although lean mass eventually rebounded in CR-fed mice (Fig. 1c and Supplementary Table 2b).

Fasting is required for CR-induced insulin sensitivity. Improved regulation of blood glucose is a conserved mammalian response to CR[1]. We examined the contribution of fasting and energy restriction on glucose homeostasis by performing glucose and insulin tolerance tests (Fig. 1f,g and Extended Data Fig. 1b,c), timing the assays such that mice in all groups were fasted for similar lengths of time. We found that all three restricted diets improved glucose tolerance after 9 weeks on the diet (Fig. 1f) and similarly after 13 weeks on the diet (Extended Data Fig. 1b). Surprisingly, we observed that insulin sensitivity as assessed by intraperitoneal insulin tolerance test was significantly improved only in mice fed the classic CR diet, and not in Diluted AL-fed or MF.cr-fed mice (Fig. 1g and Extended Data Fig. 1c). Improved glucose tolerance was not due to increased insulin secretion, and the calculated homeostatic model assessment of insulin resistance (HOMA-IR) did not differ significantly between groups (Extended Data Fig. 1d–f). These results suggest that fasting, and not a reduction in energy intake, mediates the improved insulin sensitivity of CR-fed animals.

Distinct fuel source utilization in calorie restriction is driven by fasting. CR-fed mice engage in rapid lipogenesis following refeeding, then sustain themselves via the utilization of these stored lipids[7,16]. We placed mice in metabolic chambers, allowing us to determine substrate utilization by examining the respiratory exchange ratio (RER). RER is calculated from the ratio of O_2 consumed and CO_2 produced; a value close to 1.0 indicates that carbohydrates are primarily utilized for energy production, while a value approaching 0.7 indicates that lipids are the predominant energy source[27]. An RER > 1.0 reflects the utilization of carbohydrates for active de novo lipogenesis[16]. AL and Diluted AL-fed mice had ad libitum access to food while in the metabolic chambers; CR and MF.cr mice were fed at the same time at the beginning of the light cycle while in the chambers, as technical limitations made feeding the MF.cr mice multiple times during the dark cycle impractical. We observed that RER rapidly rose above 1.0 following refeeding, and then fell below 0.8 during the dark cycle, a fuel source utilization pattern clearly distinct from that of AL-fed mice (Fig. 1h). Calculating fatty acid and carbohydrate/protein oxidation[16], we find that CR and MF.cr diets, but not the Diluted AL diet, increased fatty acid oxidation (Fig. 1i).

We examined the contribution of fasting and calories to energy expenditure (Supplementary Fig. 1a), correcting for differences in lean mass (Fig. 1j) and body weight (Supplementary Fig. 1b) using analysis of covariance (ANCOVA). As expected, mice consuming fewer calories had decreased energy expenditure relative to AL-fed mice; this effect was dependent on feeding regimen and not body weight. CR-fed and MF.cr-fed mice were more active immediately preceding and following feeding (Supplementary Figs. 1c–e); however, as activity accounts for only about 10% of mouse energy expenditure[28], the decreased energy intake of these mice is likely the primary factor in the reduced energy expenditure. These results suggest that fasting, and not a reduction in calories, is responsible for the altered fuel utilization of CR-fed animals, while the reduction in calories results in an overall decrease in energy expenditure.

Fasting is necessary for the distinct molecular signature of calorie restriction. We performed metabolomics on the livers of AL-fed, CR-fed and Diluted AL-fed mice (Extended Data Fig. 2), targeting 59 metabolites in three broad groups based on their chemical structures: amino acids, carbohydrates and nucleoside/nucleotides. We analysed CR-fed mice under two feeding conditions. First, we collected tissues from CR mice that were fed 22 h previously (CR-fasted), while AL and Diluted AL groups were fed ad libitum overnight, and food was removed in the morning 4 h before euthanasia, similar conditions as those described in the literature[21]. We also collected tissues from CR mice fed at the start of the light cycle for 3 h before euthanasia (CR-fed).

We identified 18 metabolites significantly altered in classical CR-fasted mice as compared to AL-fed mice; in contrast, we observed no differences between Diluted AL-fed mice and AL-fed mice (Extended Data Fig. 2a and Supplementary Table 3). The metabolomic signatures of CR-fasted mice were also distinct from those of AL and Diluted AL-fed mice, while the latter two groups overlapped (Extended Data Fig. 2b). The metabolomic signatures

Fig. 1 | Prolonged fasting is required for the CR-mediated increase in insulin sensitivity and alterations in fuel source selection in male C57BL/6J mice. **a**, Outline of feeding regimens (AL, Diluted AL, CR and MF.cr). **b**–**e**, Body composition measurement over 16 weeks on the diet ($n = 10$ biologically independent mice per diet): total body weight (**b**), lean mass (**c**), fat mass (**d**) and adiposity (**e**). **f**,**g**, Glucose tolerance test (GTT; AL, $n = 12$; Diluted AL, $n = 10$; MF.cr, $n = 11$; CR, $n = 11$ biologically independent mice; **f**) and insulin tolerance test (ITT; AL, $n = 11$; Diluted AL, $n = 9$; MF.cr, $n = 8$; CR, $n = 9$ biologically independent mice; **g**) after 9 or 10 weeks on the indicated diets. An asterisk represents a significant difference versus AL-fed mice ($P < 0.0001$) based on Tukey's test after one-way analysis of variance (ANOVA). **h**–**j**, Metabolic chamber analysis of mice fed the indicated diets. **h**, RER versus time ($n = 10$ biologically independent mice per diet). **i**, Fuel utilization was calculated for the 24-h period following the indicated (arrow in **h**) refeeding time ($n = 10$ biologically independent mice per diet). An asterisk represents a significant difference versus AL (Diluted AL, $P < 0.0001$; MF.cr, $P \leq 0.0018$; CR, $P \leq 0.0002$), and a hash symbol represents a significant difference versus Diluted AL (MF.cr, $P = 0.0097$; CR, $P \leq 0.0283$) based on Tukey's test after one-way ANOVA performed separately for fatty acid oxidation (FAO) and carbohydrate/protein oxidation (C/PO). **j**, Energy expenditure (EE) as a function of lean mass was calculated for the 24-h period following the indicated (arrow in **h**) refeeding time ($n = 10$ mice per diet; data for each individual mouse are plotted, and slopes and intercepts were calculated using ANCOVA). All data are presented as the mean ± s.e.m. AUC, area under the curve.

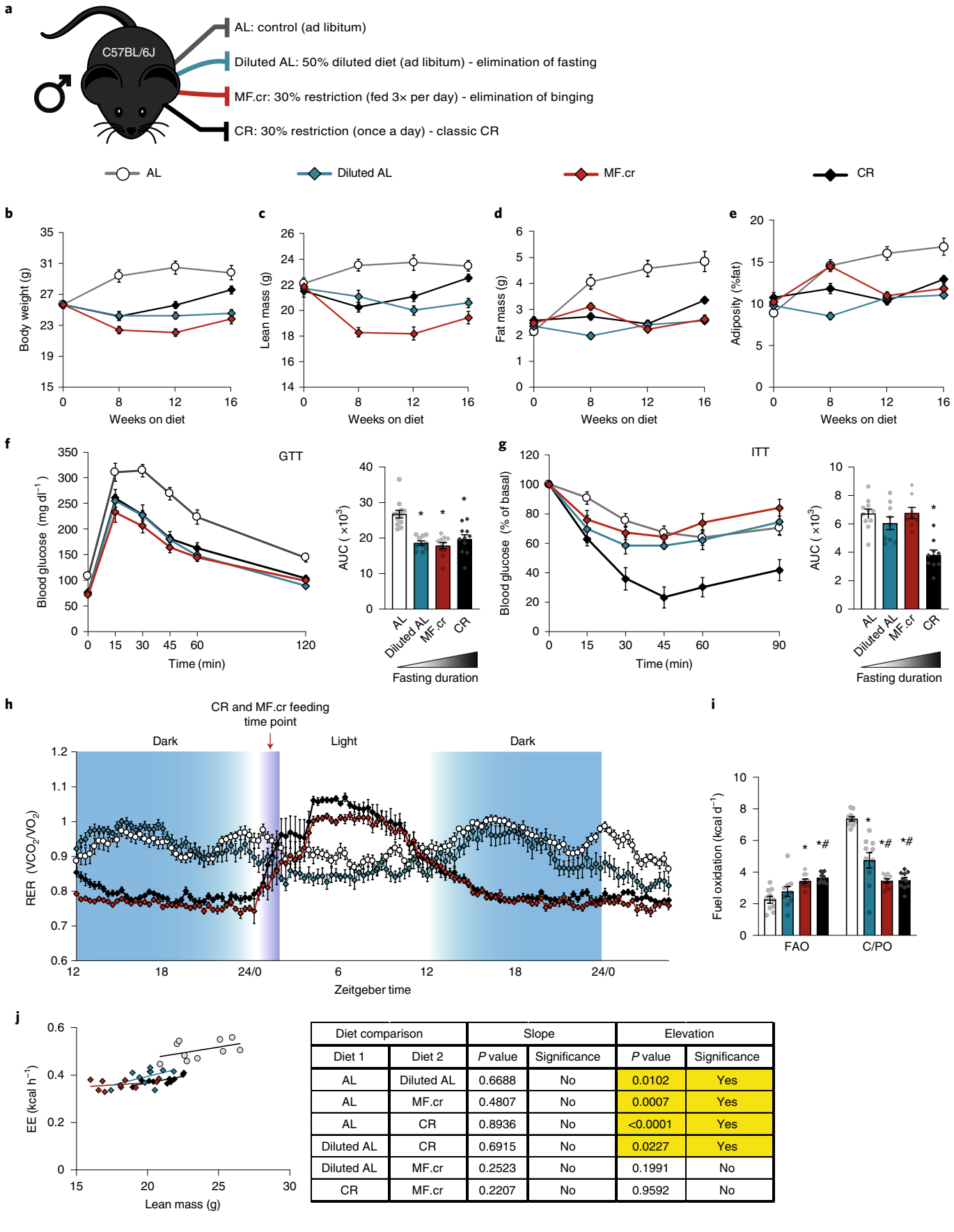

Diet comparison		Slope		Elevation	
Diet 1	Diet 2	*P* value	Significance	*P* value	Significance
AL	Diluted AL	0.6688	No	0.0102	Yes
AL	MF.cr	0.4807	No	0.0007	Yes
AL	CR	0.8936	No	<0.0001	Yes
Diluted AL	CR	0.6915	No	0.0227	Yes
Diluted AL	MF.cr	0.2523	No	0.1991	No
CR	MF.cr	0.2207	No	0.9592	No

of CR-fed mice were metabolically distinct from AL-fed mice (Extended Data Fig. 2a,c), suggesting that CR-fed animals have distinct liver metabolomic signatures from AL-fed mice regardless of feeding state. Nucleotides/nucleosides and metabolites involved in carbohydrate metabolism were more substantially altered in the fasted than the fed state, with the exception of alpha-ketoglutarate (Extended Data Fig. 3a,b). We found broad changes in amino acid metabolism, with leucine, ornithine and proline significantly elevated in both CR-fasted and CR-fed groups relative to AL-fed controls (Extended Data Fig. 3c). Additionally, three amino acids—lysine, isoleucine and tryptophan–trended upwards in CR-fasted mice and were significantly elevated in CR-fed mice (Extended Data Fig. 3c).

Intriguingly, levels of methionine and *S*-adenosylhomocysteine, a metabolite of *S*-adenosylmethionine-consuming methyltransferase reactions, were elevated in the livers of CR mice (Extended Data Fig. 2d). Changes in levels of methionine and methionine metabolites can result in epigenetic changes, altering global histone post-translational modifications (PTMs)[29,30]. We observed changes in global histone PTMs in the livers of both Diluted AL and CR-fed mice, with the CR diet resulting in a greater number of significantly altered histone PTMs (Extended Data Fig. 4 and Supplementary Table 4). CR-fed mice possessed a distinct histone PTM profile compared to that of AL-fed and Diluted AL-fed mice, which were more similar to each other (Extended Data Fig. 4a,b). Restriction of calories non-specifically increased acetylated histone H3 and non-specifically decreased acetylated histone H4 (Extended Data Fig. 4c). Tri-methylated histone H3 at Lys27 (H3K27), a modification strongly associated with chromatin silencing[31], increased in CR-fed mice; di-methylated histone H3 at Lys9 (H3K9) decreased, while acetylated H3K9/Lys14 increased. Our results suggest that prolonged fasting, not simply a reduction of calorie intake, is required for the epigenetic effects of a CR diet.

We also conducted targeted metabolomics in skeletal muscle[32–37] (Extended Data Fig. 5 and Supplementary Table 5). We found many metabolites were altered in both CR-fed mice and Diluted AL-fed mice as compared to AL-fed controls (Extended Data Fig. 5a). CR-fed mice had a distinct metabolomic signature from AL-fed mice; however, unlike in the liver, Diluted AL-fed mice had a distinct signature from AL-fed mice (Extended Data Fig. 5b). CR and Diluted AL-fed mice had similar changes in multiple tricarboxylic acid (TCA)-cycle metabolites with the exception of malate and 2-hydroxyglutarate. Although prolonged fasting is required to produce the distinct metabolomic signature of CR in both the liver and skeletal muscle, reduction of calories also affects the skeletal muscle metabolome.

Sex and strain response to fasting and calories. Sex and genetic background impact the response to CR in mice[21,22,26]. To determine if the distinct roles of calorie and fasting we observed in B6M mice was conserved across different sexes and strains, we examined female C57BL/6J (B6F) mice, and male and female DBA/2J (D2M and D2F) mice (Extended Data Figs. 6–8). These strains have different metabolic responses to once-daily CR, but CR extends the lifespan of both strains and sexes[21].

All three dietary regimens had similar effects on the body composition of B6M and D2M mice (Fig. 1b–e and Extended Data Fig. 7b–e). While female B6F and female D2F mice gained less weight on all of the reduced-calorie regimens, Diluted AL-fed female mice did not gain fat mass nor adiposity (Extended Data Figs. 6a–d and 8a–d), suggesting there may be a sexually dimorphic effect of fasting (or the lack thereof) on fat storage. Glucose tolerance was improved by the reduced-calorie regimens in all sexes and strains, with the exception of B6F mice that were fed the classical CR diet (Fig. 1f, Extended Data Figs. 6f–8f and Supplementary Fig. 2a). While the non-responsiveness of B6F mice was somewhat surprising, these findings were in line with our previous observation that the effect of CR on glucose tolerance is stronger in young male mice than in young female mice[7]. This was not due to increased insulin secretion (Supplementary Fig. 3).

Insulin sensitivity as assessed by insulin tolerance test using 0.5 U per kg of body weight of insulin was significantly improved only in B6M mice that were fed the classic CR diet, and B6F mice fed either the classic CR diet or the MF.cr diet (Fig. 1g, Extended Data Fig. 6g and Supplementary Fig. 2b). We did not observe improved insulin sensitivity in response to any of the restricted diets for DBA/2J mice of either sex under these conditions (Extended Data Figs. 7g and 8g), exemplifying the genetic variation in response to insulin between strains[38]. As these mice were less responsive to insulin, after 14 weeks on the diet, we challenged both male and female DBA/2J mice with a higher dose of insulin (0.75 U per kg of body weight) to uncover differences between the diet regimens. We observed improved insulin sensitivity in D2F mice fed the classic CR diet, but not in D2M mice (Supplementary Fig. 2b). In all sexes and strains, mice fed the Diluted AL diet did not have significantly improved insulin sensitivity, despite the reduction in caloric intake. Interestingly, the Diluted AL group had the smallest HOMA-IR value for B6F and D2M (Supplementary Fig. 3). These data demonstrate that sex and strain impact the effect of different CR regiments on glucose homeostasis.

Using metabolic chambers, we determined the RER and energy expenditure and calculated substrate utilization of all sexes, strains and diet groups. All mice fed a classic CR diet had similar RER patterns to those of B6M, rapidly rising above 1.0 following refeeding and then falling to ~0.7–0.8 during the dark cycle (Fig. 1h and Extended Data Figs. 6h–8h). While all mice fed the MF.cr diet had similar RER curves to classic CR-fed mice, all mice fed the Diluted AL diet had RER curves that overlapped those of the AL group (Extended Data Figs. 6h–8h). As in B6M mice, CR and MF.cr diets increased fatty acid oxidation in D2M and D2F mice; B6F fed either one of these diets had fatty acid oxidation indistinguishable from AL-fed controls (Fig. 1i and Extended Data Figs. 6i–8i), suggesting that the strain-specific and sex-specific responses to CR regimens extend to fat metabolism. In contrast, fatty acid oxidation was not increased in Diluted AL-fed mice of any sex or strain.

All mice consuming fewer calories had decreased energy expenditure relative to their AL-fed counterparts; this effect was independent of both fat-free (lean) mass and body weight (Fig. 1j, Extended Data Figs. 6j–8j and Supplementary Fig. 4). While all restricted groups of C57BL/6J and DBA/2J males had similar energy expenditure, female mice of both strains fed the diluted diet had lower energy expenditure compared to both CR and MF.cr-fed mice (Extended Data Figs. 6j and 7j). These results suggest that fasting is responsible for the altered fuel utilization of CR-fed animals, while the reduction in calories is responsible for the decreased energy expenditure.

The physiological responses to these restricted paradigms were differentially regulated by strain and sex. To visualize the overall response, we plotted 17 phenotypes calculated relative to the AL control. We first plotted how each individual sex/strain of mice responded to the three dietary regimens (Fig. 2a–d). Secondly, we plotted how all four strains responded to each individual diet (Fig. 2e–g). To identify statistically significant interactions of sex, strain and diet, we performed multivariate statistical analyses on the 17 phenotypes. We used two-way ANOVA corrected for multiple comparisons by false discovery rate (FDR) using the two-stage linear step-up procedure of Benjamini, Krieger and Yekutieli; the q values (FDR) and individual P values are shown in Supplementary Table 6. The majority of the phenotypic outcomes were both strain and sex dependent. In particular, D2F mice exhibited higher insulin sensitivity than D2M mice, and B6F mice exhibited higher insulin sensitivity than D2F mice. For fatty acid oxidation there was a

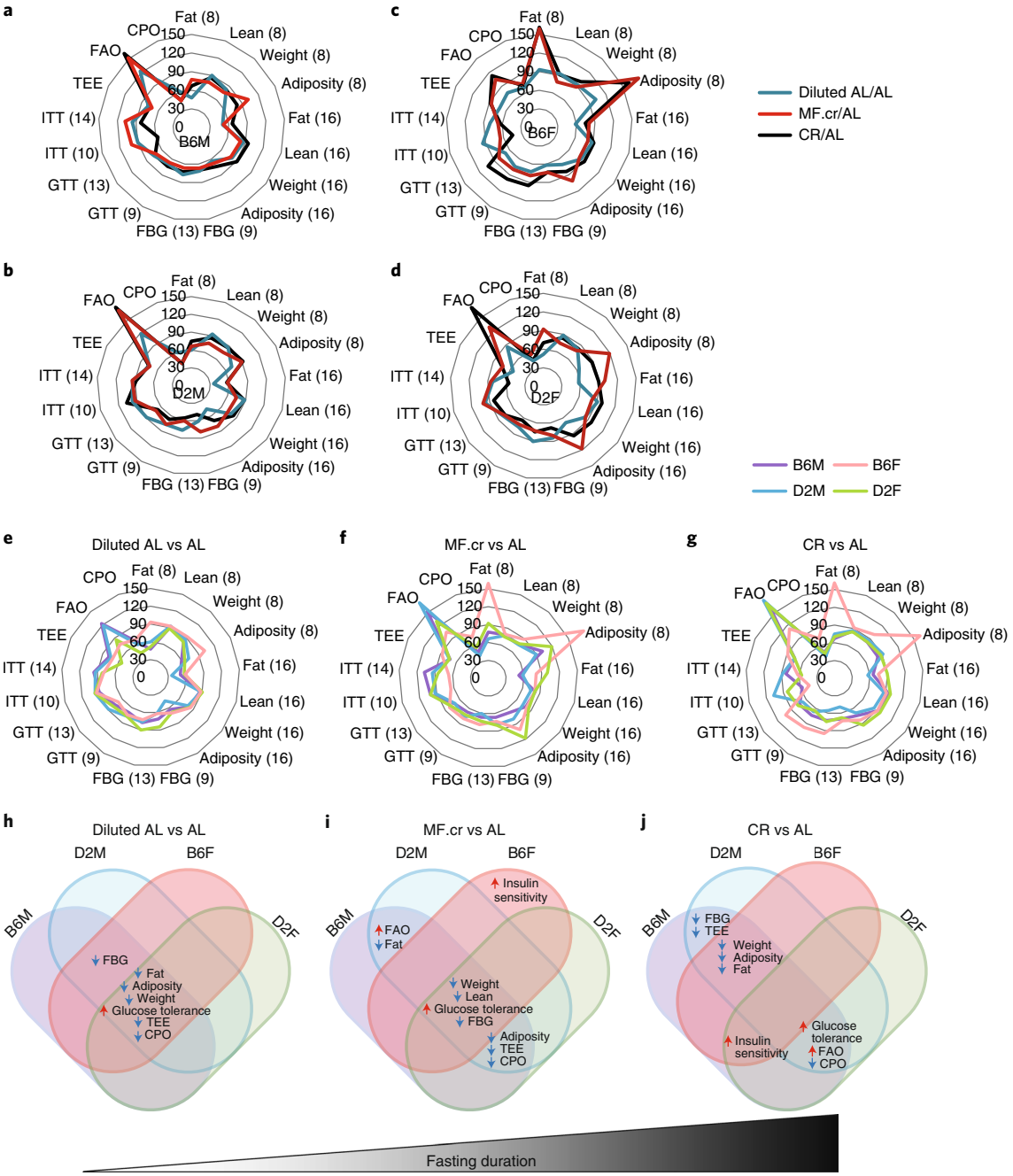

Fig. 2 | Distinct physiological responses to diet in different strains and sexes of mice. a–g, Radar charts of 17 phenotypes measured in C57BL/6J and DBA/2J male and female mice while consuming the indicated diets. **a–d**, The distance from the centre represents the effect of each restricted diet versus AL-fed mice (0–150 min; no difference = 100%; blue, Diluted AL; red, MF.cr; black, CR). **e–g**, The distance from the centre represents the effect of Diluted AL-fed versus AL-fed mice (**e**), MF.cr-fed versus AL-fed mice (**f**) and CR-fed versus AL-fed mice (**g**) for the indicated strain and sex (no difference = 100%). FBG, fasting blood glucose; TEE, total energy expenditure. The computed AUC was derived from the GTT and ITT. The number in parentheses refers to the number of weeks on the diet for each phenotype. **h–j**, Summary comparison of diet effect on phenotypes compared to AL for each strain and sex.

sex–diet interaction for DBA/2J mice, and a strain–diet interaction for both sexes. When total energy expenditure was evaluated against each strain and sex with ANCOVA, there were only strain differences for AL-fed, Diluted AL-fed and MF.cr-fed mice. However, there were both strain and sex interactions for CR-fed mice.

Overall, there was little difference with strain or sex when only calories were restricted (Fig. 2h). As fasting duration increased, we observed an increasing number of sex and strain differences (Fig. 2i,j). Our data support the idea that each sex and strain respond to a CR diet uniquely as a result of sex-specific and strain-specific responses to prolonged fasting.

Fasting recapitulates the metabolic effects of a CR diet. We next wanted to examine the possibility that fasting is sufficient to recapitulate the metabolic and molecular effects of a classical once-per-day CR diet. We designed a fifth feeding paradigm, TR.al, in which B6M

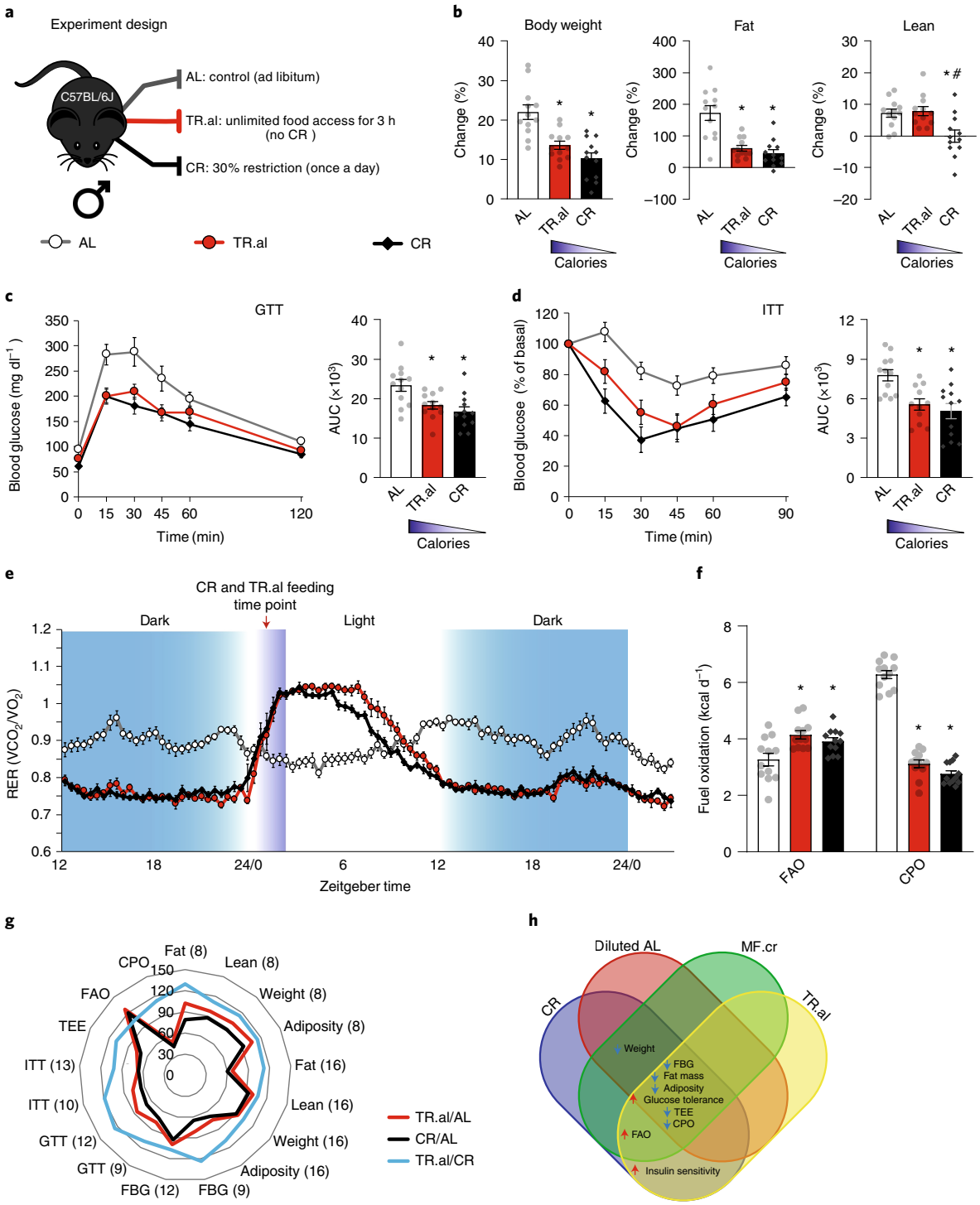

Fig. 3 | Fasting alone recapitulates the metabolic effects of a CR diet. a, Schematic of feeding paradigms: AL, TR.al and CR. **b**, Changes in body weight, fat and lean mass over the course of 16 weeks consuming the indicated diets ($n = 12$ biologically independent mice per diet). **c**,**d**, A glucose tolerance test (**c**; $n = 12$ biologically independent mice per diet; an asterisk represents a significant difference versus AL-fed mice: TR.al, $P = 0.0204$; CR, $P = 0.0019$; based on Tukey's test after one-way ANOVA) and an insulin tolerance test (**d**; AL, $n = 12$; TR.al, $n = 11$; $n = 8$; CR, $n = 12$ biologically independent mice; an asterisk represents a significant difference versus AL-fed mice: TR.al, $P = 0.0086$; CR, $P = 0.0010$; based on Tukey's test after one-way ANOVA) were conducted after mice were fed the indicated diets for 9 or 10 weeks, respectively. **e**, RER versus time ($n = 12$ biologically independent mice per diet). **f**, Fuel utilization was calculated for the 24-h period following the indicated (arrow in **e**) refeeding time ($n = 12$ biologically independent mice per diet; an asterisk represents a significant difference versus AL: TR.al, $P \leq 0.0027$; CR, $P \leq 0.0306$; based on Tukey's test after one-way ANOVA performed separately for FAO and C/PO). **g**, Radar chart of 17 phenotypes measured in male C57BL/6J mice consuming the indicated diets. **h**, Comparison of diet effects on the phenotypes of C57BL/6J male mice for all feeding regimens examined in this paper. All data are presented as the mean ± s.e.m.

mice were entrained to consume approximately the same quantity of food as ad libitum-fed mice within 3 h (Fig. 3a and Extended Data Fig. 9a), following which they were fasted for the remaining 21 h of each day.

We found that both classical CR-fed mice and TR.al-fed mice had reduced overall weight and fat mass gain during the 16 weeks of the study, despite the similar calorie intake of AL-fed and TR.al-fed mice (Fig. 3b, Extended Data Figs. 9a–e and Supplementary Table 7). Additionally, TR.al-fed mice had improved glucose tolerance and insulin sensitivity after 9–10 weeks (Fig. 3c,d). These early improvements in glucose homeostasis were independent of substantial differences in weight and adiposity, which only diverged after 12 weeks on the diet (Extended Data Fig. 9b–e). Glucose tolerance and insulin sensitivity were similarly improved after 13–14 weeks on the diets (Extended Data Fig. 9f,g), and were not the result of increased insulin secretion (Extended Data Fig. 9h–j). These results demonstrate that prolonged fasting is sufficient to improve body composition, glucose tolerance and insulin sensitivity.

We utilized metabolic chambers to determine substrate utilization and energy expenditure. As previously shown, we found that classic CR-fed mice exhibited two distinct phases of fuel selection following feeding, with high lipogenesis (RER > 1.0) following feeding, and dependence on lipid oxidation (RER < 0.8) during the dark cycle, and an overall increase in fatty acid oxidation (Fig. 3e,f). TR.al-fed mice were essentially indistinguishable from classic CR-fed mice, with overlapping RER curves and similar increases in fatty acid oxidation (Fig. 3e,f). The CR and TR.al groups both demonstrated decreased total energy expenditure relative to AL-fed mice that was independent of lean (fat-free) mass and body weight (Supplementary Fig. 5).

Almost all of the metabolic phenotypes of CR-fed mice were also observed in TR.al-fed mice (Fig. 3g). Additionally, when comparing all the feeding paradigms examined for B6M mice, we observed that only mice subjected to prolonged fasting, that is, the CR and TR.al groups, showed improved insulin sensitivity, while any length of fasting was sufficient to increase fatty acid oxidation (Fig. 3h). Together, these results demonstrate that fasting recapitulates the physiological response to CR, and is both necessary and sufficient for the metabolic response to CR.

Fasting recapitulates the molecular effects of a CR diet. We next performed transcriptomic profiling of liver tissue and inguinal white adipose tissue (iWAT) of mice fed the AL, CR or TR.al diet. We identified 2,700 genes in the liver and more than 1,800 genes in iWAT that were differentially expressed ($q < 0.05$) in either CR or TR.al-fed mice relative to AL-fed mice (Fig. 4a–c and Supplementary Tables 8 and 9). A large fraction of these genes was altered in the same direction by both CR and TR.al feeding (Fig. 4b), and over 90% of the differentially expressed genes (DEGs) were the same in iWAT and liver of CR and TR.al animals (Fig. 4c).

We next took an unbiased approach in identifying functionally enriched pathways by constructing gene-set networks with NetworkAnalyst[39–43]. DEGs were assigned as 'seed' proteins and pathways were constructed with the known interactions of the seed protein with other proteins curated from a large protein–protein interaction database (Fig. 4d,e). From this, we identified likely candidate pathways mediating these responses by limiting pathway hits with enrichment P values < 0.05, calculated with the hypergeometric test, which is an enrichment analysis test that calculates for significant overlap between genes, and ranked all the genes by their P values.

More pathways were altered in iWAT than in the liver. We identified 25 upregulated pathways in iWAT that were functionally enriched in tissues from both CR-fed and TR.al-fed mice (Fig. 4f). In liver, we identified five upregulated and five downregulated pathways that were functionally enriched by both diets (Fig. 4g). Additionally, some pathways were enriched in tissues for both CR-fed and TR.al-fed mice, but reached statistical significance only for one diet, such as the mechanistic target of rapamycin (mTOR) signalling pathway in iWAT (Fig. 4f) or peroxisome proliferator-activated receptor (PPAR) signalling in liver (Fig. 4g). Lastly, we examined the similarities of enriched pathways between iWAT and liver. We identified six pathways upregulated in both tissues by both CR and TR.al diets: 'insulin signalling pathway', 'PPAR signalling pathway', 'fatty acid biosynthesis', 'circadian rhythm', 'metabolic pathways' and 'fatty acid metabolism' (Fig. 4f,g). We also identified two additional pathways that were upregulated in both tissues by TR.al only: 'transforming growth factor (TGF)-β signalling pathway' and 'longevity-regulating pathway' (Fig. 4f,g). Finally, we found two pathways that were regulated in opposite directions in liver and iWAT by a TR.al diet: 'signalling pathways regulating pluripotency of stem cells' and 'MAPK signalling pathway' (Fig. 4f,g).

Fasting is necessary for calorie restriction to improve health and longevity. To understand the requirement for fasting in the effects of a CR diet on ageing, we placed 20-week-old C57BL/6J male mice on the AL, Diluted AL or CR diet (Fig. 5a), and measured weight, body composition, glucose homeostasis, gut integrity and frailty as the animals aged (Fig. 5 and Extended Data Fig. 10). As we expected, mice fed the classical CR diet ceased to gain weight, fat mass and lean mass, and maintained a lower adiposity than AL-fed controls (Fig. 5b). In contrast, Diluted AL-fed mice had an initial reduction in body weight and fat mass and started to steadily lose lean mass at 9 months of age (Fig. 5b, Extended Data Fig. 10a and Supplementary Table 10). To determine if cellulose in the Diluted AL diet impairs the absorption of energy-yielding nutrients, we assessed the gross energy in diet consumed and faeces excreted by bomb calorimetry of 19-month-old mice. Diluted AL-fed mice ate more and had increased faecal output; when accounting for the amount of cellulose consumed, Diluted AL-fed mice absorbed digestible macronutrients similarly to AL-fed mice (Extended Data Fig. 10b). We additionally checked if gut barrier integrity was affected by the Diluted AL diet with fluorescein isothiocyanate-dextran (FITC-dextran, 4 kDa) in 20-month-old mice. While Diluted AL-fed animals had the same level of permeability as the AL group, CR-fed animals had improved gut barrier integrity (Extended Data Fig. 10c).

We assessed glucose and insulin tolerance as the mice aged; both diets improved glucose tolerance (Fig. 5c,e), while insulin sensitivity was only improved in the classical CR-fed group (Fig. 5d,f). As in young animals, classical CR-fed mice displayed a distinctive RER curve, with a rapid induction of lipogenesis (RER > 1.0) following refeeding, and a low RER throughout the night (Fig. 5g). We calculated that CR-fed mice utilized fatty acids as a fuel source significantly more throughout the day compared to other groups (Fig. 5h). CR and Diluted AL groups both demonstrated decreased total energy expenditure relative to AL-fed mice that was independent of non-fat mass or total body weight with no significant differences in activity between groups (Supplementary Fig. 6).

We assessed the frailty of AL, Diluted AL and CR-fed mice as they aged. As expected[7,44], frailty was significantly lower in CR-fed mice as they aged (Fig. 6a). In contrast, frailty was not reduced in Diluted AL-fed mice (Fig. 6a). Intriguingly, the specific deficits of AL-fed and Diluted AL-fed mice that contributed to their equivalent frailty varied, with Diluted AL-fed mice developing kyphosis, and AL mice having declining grip strength and body composition (Fig. 6b–e). The quality of the coat condition and fur colour were diminished in both AL and Diluted AL mice, while CR mice retained a healthy coat (Fig. 6f,g). Additionally, we examined if fasting was required for cognition and memory by testing novel object recognition[45]. Short-term memory was not improved in either Diluted AL-fed or CR-fed mice; however, classic once-per-day CR feeding, but not a Diluted AL diet, improved long-term memory

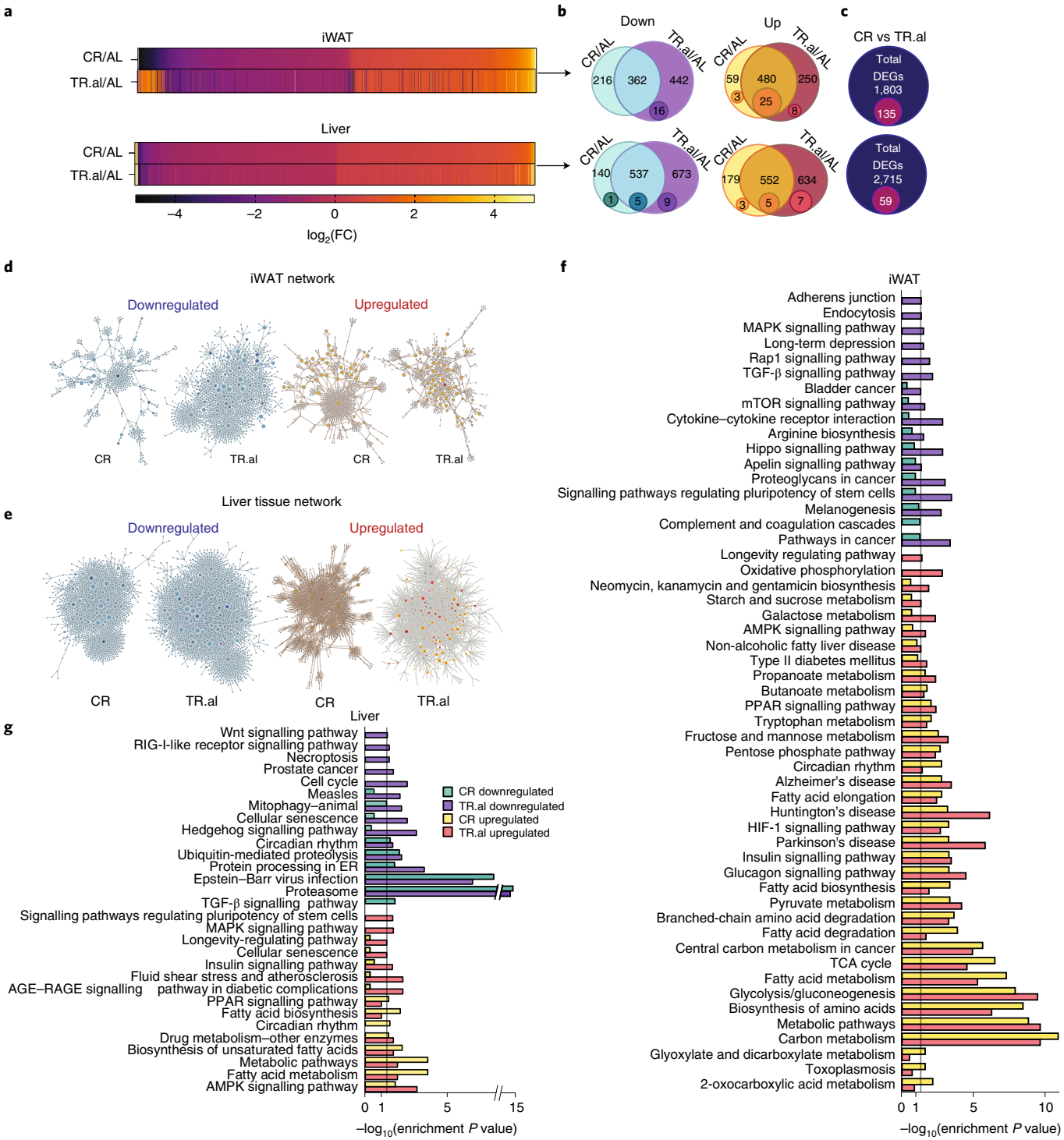

Fig. 4 | Fasting and calorie restriction result in highly similar transcriptomic signatures in liver and white adipose tissue. Transcriptional profiling was performed on liver and iWAT from mice fed the AL, CR or TR.al regimen ($n = 6$ per diet group). **a**, Heat map of differently expressed genes of CR and TR.al-fed mice compared to AL-fed mice in liver and iWAT. **b**,**c**, Overlap between DEGs in CR-fed mice and TR.al-fed mice relative to AL-fed mice. Numbers in Venn diagrams represent the number of genes (large circle) and functionally enriched pathways (small circle) identified from network construction in **d** and **e**. **d**,**e**, Network construction of significantly upregulated and downregulated genes of CR and TR.al groups in iWAT (**d**) and liver (**e**) using NetworkAnalyst. Node size represents number of edges connected to a node and the colours represent directionality of enrichment. Downregulated: green, CR specific; light blue, CR and TR.al, $P < 0.05$; dark blue, CR and TR.al, with only TR.al $P < 0.05$; purple, TR.al specific $P < 0.05$, grey, edges and unknown nodes. Upregulated: yellow, CR specific; orange, CR and TR.al, $P < 0.05$; dark orange, CR and TR.al, with only TR.al $P < 0.05$; red, TR.al specific $P < 0.05$; grey, edges and unknown nodes. **f**,**g**, Significantly upregulated and downregulated pathways identified from network construction in iWAT (**f**) and liver (**g**). Bar graphs represents pathways identified enriched in CR and/or TR.al-fed mice with enrichment $P < 0.05$ as computed with the hypergeometric test. ER, endoplasmic reticulum.

(Fig. 6h,i), suggesting that fasting may play a role in the effects of a CR diet on cognition.

Finally, we analysed the survival of the mice on the three different diets as they aged. While classic once-per-day CR feeding extended lifespan by about 20% (AL versus CR, median lifespan 850 d versus 1,022 d, $P<0.0001$ versus AL, log-rank sum test), consumption of the Diluted AL diet decreased lifespan by 9% (AL versus Diluted AL, median lifespan 850 d versus 776 d, $P<0.0001$ versus AL, log-rank sum test; Fig. 6j and Supplementary Table 11). Additionally, CR delayed the onset of cancer compared to AL, while the incidence of cancer in Diluted AL-fed mice was low, perhaps due to their shorter lifespan (Fig. 6k). In combination, our data suggest that fasting is required for the geroprotective effects of CR on frailty, cognition and lifespan (Fig. 6l).

Discussion

The mechanisms by which CR promotes health span and longevity have remained elusive for decades. Most CR studies have overlooked that a traditional once-per-day feeding regimen alters feeding behaviour[15,16]. Meal feeding, which imposes a fasting period, was recently shown to extend lifespan without restricting caloric intake[20,46], which suggested to us that the fasting period collaterally imposed by a conventional once-per-day CR feeding regimen might be a critical and hitherto overlooked physiological mechanism contributing to the effects of CR.

We tested this hypothesis by using a new series of feeding regimens. We found that a reduction of calories without the imposition of a prolonged fast improves glucose tolerance and body composition. However, prolonged fasting was necessary for CR to improve insulin sensitivity, a key physiological hallmark of the CR response in mammals; alter fuel utilization patterns and increase fatty acid oxidation; and reduce age-related frailty[6,7,16,44,47,48]. Of note, we assessed insulin sensitivity via intraperitoneal administration of insulin, which most directly measures insulin-stimulated glucose uptake; future research using clamps may be useful in thoroughly assessing the insulin sensitivity of other tissues including the liver.

C57BL/6J male mice in which calorie intake was reduced without fasting via ad libitum feeding of a low-energy diet did not show the anticipated reduction in age-related frailty, and had a reduced lifespan. Our findings align with the results of other laboratories[8], and with the results of our molecular analysis of the liver, which likewise showed that restriction of calories without fasting had a distinct and muted impact on metabolites and histone PTMs as compared to mice fed a CR diet once per day. We observed changes in multiple methionine metabolites, and while it is difficult to directly compare metabolomics data across studies, other groups have seen similar changes[21,46,49–52]. In agreement with another study of mice fed the same chow we used[21,46], we observed that CR increased levels of leucine and isoleucine in the liver.

Our use of a diet diluted with indigestible cellulose (Diluted AL) is a limitation of the present work, as the large bulk of fibre in this diet may have affected the gut microbiome and impacted the metabolic effects we observed. While the diet did not affect macronutrient absorption or gut integrity, absorption of specific micronutrients was not investigated. We examined the effect of a more 'normal' CR diet, delivered in multiple meals (MF.cr), only in our short-term studies. Future studies examining different MF.cr lengths in longer studies, testing multiple feeding times, and examining macronutrient and micronutrient absorption will permit a more complete understanding of how the length of time between meals contributes to the effects of a CR diet. This may also clarify why some studies report positive effects of cellulose-diluted diets on lifespan[53], and explain why dilution of specific macronutrients extends the lifespan of other model organisms[14,54–56].

Not only is a fasting period necessary, but the imposition of a prolonged daily fast without reduced calories recapitulates the metabolic benefits and molecular effects of a CR diet in C57BL/6J male mice. Fasting improves glucose tolerance and insulin sensitivity, reduces adiposity and increases fatty acid oxidation. At the molecular level, fasting and traditional CR had extremely similar and overlapping effects on gene expression, with high similarity in the pathways altered by fasting and CR. Fasting almost completely recapitulates the effects of CR in both liver and iWAT, both in terms of DEGs and in Kyoto Encyclopedia of Genes and Genomes (KEGG) pathways. Notably, many of the KEGG pathways identified as altered by both fasting and CR have been previously implicated in the metabolic and geroprotective effects of a CR diet; these include PPAR, insulin, TGF-β and AMPK signalling, as well as multiple metabolic pathways involved in amino acid, carbohydrate and fatty acid metabolism. Similar changes in amino acid metabolism, PPAR expression and TGF-β and insulin signalling have been found in recent metabolomic and transcriptomic studies of the effects of graded levels of CR[49,57,58]. Intriguingly, circadian rhythm was identified as a significantly altered pathway upregulated by both CR and fasting in iWAT, and by CR in the liver. We speculate that the daily fasting of mice on a classical CR diet may promote health and longevity in part through the circadian synchronization of metabolic processes[59]. Taken together, our data demonstrate that prolonged fasting is sufficient to recapitulate the majority of the effects of CR at the molecular level in both liver and iWAT. Additional research will be required to determine the role of these various pathways, as well as circadian regulators, in the response to prolonged fasting and CR.

Our study was subject to limitations. First, while we performed our initial sufficiency studies in multiple strains and sexes of

Fig. 5 | Prolonged fasting is required for the CR-mediated increase in insulin sensitivity and fuel selection in aged mice. a, Outline of feeding paradigms: AL, Diluted AL and CR. Diets were fed to C57BL/6J male mice starting at 4 months of age. **b**, Changes in body composition (body weight, fat mass, lean mass and adiposity) were tracked longitudinally (*n* varied by days; AL, $n=12$–33; Diluted AL, $n=13$–33 mice; CR, $n=13$–33 biologically independent mice; statistics in Supplementary Table 10). **c**, Glucose tolerance test performed at 10 months of age (AL, $n=16$; Diluted AL, $n=15$; CR, $n=16$ biologically independent mice). An asterisk represents a significant difference versus AL-fed mice (Diluted AL, $P<0.0001$), and a hash symbol represents a significant difference versus Diluted AL-fed mice (CR, $P=0.0040$) based on Tukey's test after one-way ANOVA. **d**, Insulin tolerance test performed at 10 months of age (AL, $n=16$; Diluted AL, $n=12$; CR, $n=16$ biologically independent mice). An asterisk represents a significant difference versus AL-fed mice (CR, $P<0.0001$), and a hash symbol represents a significant difference versus Diluted AL-fed mice (CR, $P<0.0001$) based on Tukey's test after one-way ANOVA. **e**, Glucose tolerance test performed at 19 months of age (AL, $n=10$; Diluted AL, $n=8$; CR, $n=10$ biologically independent mice). An asterisk represents a significant difference versus AL-fed mice (Diluted AL, $P<0.0001$; CR, $P=0.0237$), and a hash symbol represents a significant difference versus Diluted AL-fed mice (CR, $P=0.0270$) based on Tukey's test after one-way ANOVA. **f**, Insulin tolerance test performed at 19 months of age (AL, $n=9$; Diluted AL, $n=8$; CR, $n=8$ biologically independent mice). An asterisk represents a significant difference versus AL-fed mice (CR, $P<0.0001$), and a hash symbol represents a significant difference versus Diluted AL-fed mice (CR, $P<0.0001$) based on Tukey's test after one-way ANOVA. **g**, RER versus time at ~15 months in age (AL, $n=29$; Diluted AL, $n=13$; CR, $n=29$ biologically independent mice). **h**, Fuel utilization was calculated for the 24-h period following the indicated refeeding time (arrow in **g**; AL, $n=29$; Diluted AL, $n=13$; CR, $n=29$ biologically independent mice). An asterisk represents a significant difference versus AL (Diluted AL, $P=0.0179$; CR, $P=0.0352$), and a hash symbol represents a significant difference versus Diluted AL (CR, $P\leq0.0001$) based on Tukey's test after one-way ANOVA performed separately for FAO and C/PO). All data are presented as the mean ± s.e.m.

mice, our metabolomic and epigenetic analysis was limited to C57BL/6J male mice on just three dietary regimens. As the effects of dietary composition and CR are sex and strain dependent[21,22,60], investigating the effects in multiple sexes and strains is critical. Our detailed studies of the effects of fasting alone were confined to C57BL/6J males, as this group showed the greatest metabolic

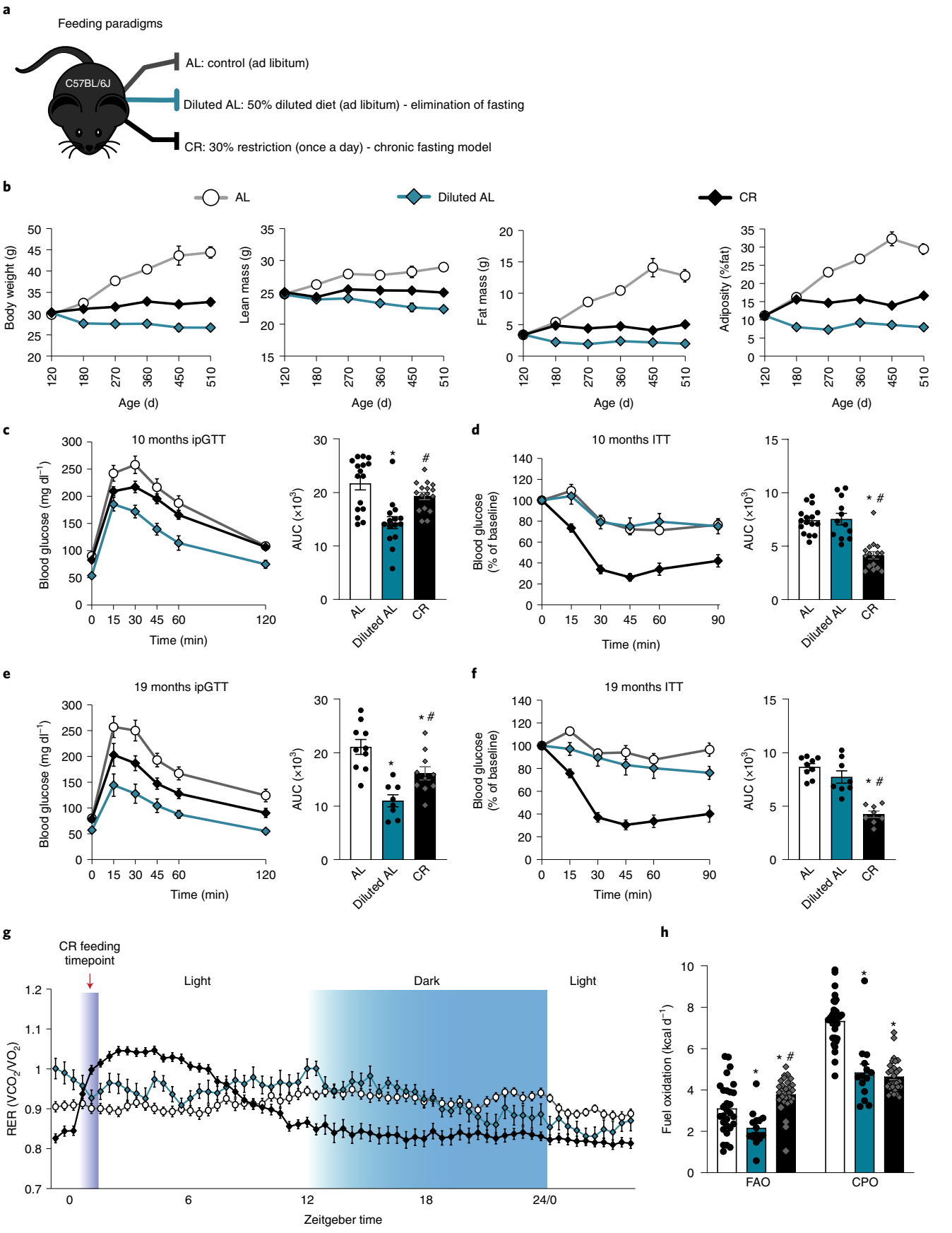

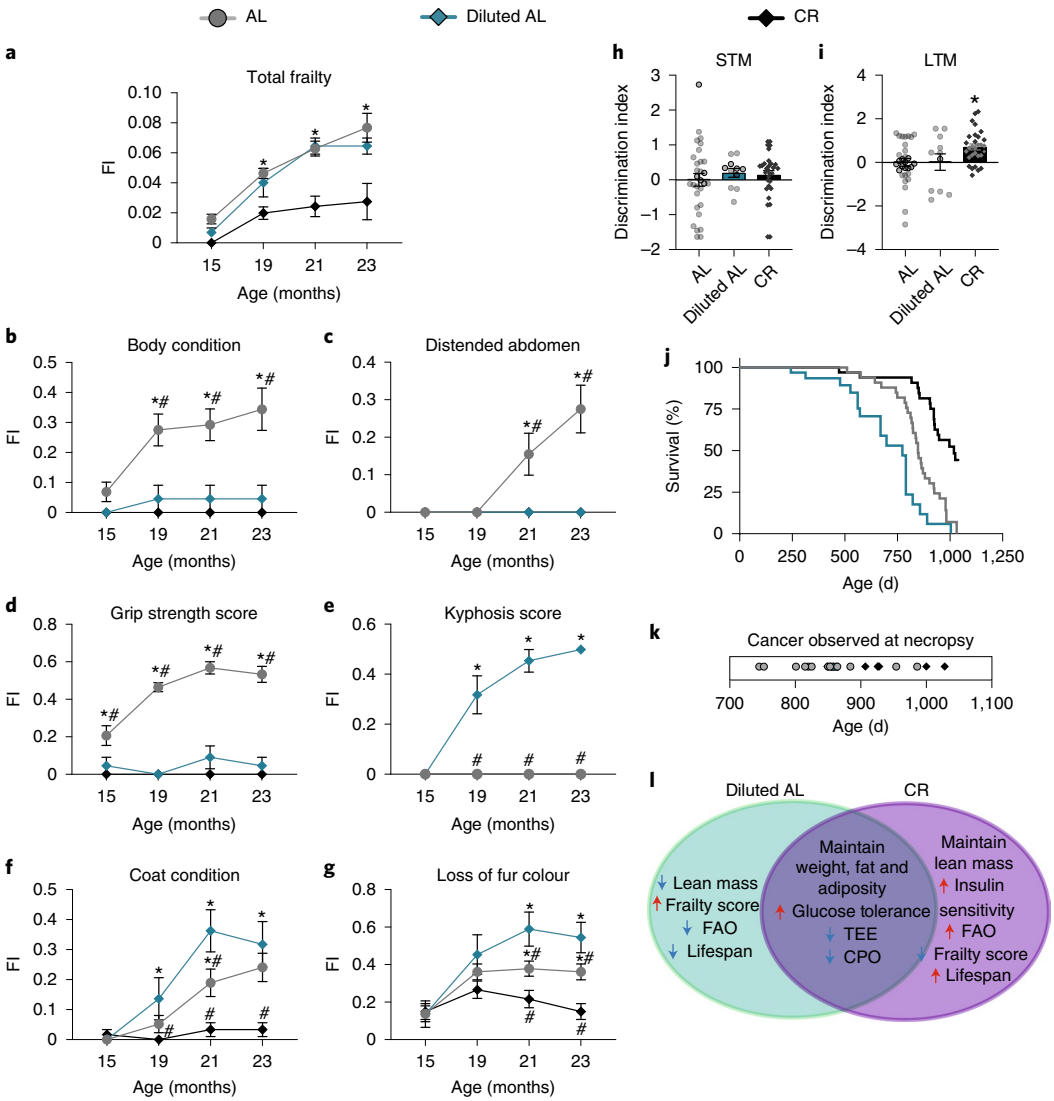

Fig. 6 | Fasting is required for the geroprotective effects of a CR diet. a–g, Frailty of mice was determined from 15–23 months of age and mice that did not survive up to 23 months of age were excluded. Total frailty (**a**) and specific deficits (**b–g**) of interests scored as part of the clinical frailty index (FI). **a–g**, AL, $n=29$; Diluted AL, $n=11$; CR, $n=30$ biologically independent mice. An asterisk represents a significant difference versus AL (CR, $P<0.0001$), and a hash symbol represents a significant difference versus Diluted AL (CR, $P<0.0001$), based on Tukey's test after two-way ANOVA. **h,i**, A novel object recognition test was performed at 21 months of age to assess short-term memory (STM; **h**) and long-term memory (LTM; **i**). AL, $n=30$; Diluted AL, $n=11$; CR, $n=30$ biologically independent mice. An asterisk represents a significant difference versus AL (CR, $P<0.0001$), and a hash symbol represents a significant difference versus Diluted AL (CR, $P<0.0001$), based on Tukey's test after two-way ANOVA. **j**, Kaplan–Meier plot of the lifespan of mice on the indicated diets starting at 4 months of age; log-rank test (Mantel–Cox), $P<0.0001$, AL versus Diluted AL and AL versus CR; log-rank test for trend, $P=0.0001$, AL versus Diluted AL and AL versus CR. **k**, Tumours observed at the time of necropsy; each dot represents a single mouse. **l**, Comparison of phenotypes induced by Diluted AL and CR diets, as compared to AL diet. All data are presented as the mean ± s.e.m.

response to a CR diet, and we focused on just a few diets for logistical reasons. Finally, TR.al-fed mice had a small reduction in calorie intake relative to AL-fed mice. We consider it unlikely that this contributes substantially to the effects of a TR.al diet, but follow-up studies should minimize or eliminate this difference. Additional research will be required to determine if fasting is sufficient to recapitulate the metabolic, molecular and geroprotective effects of a CR diet in multiple strains and sexes as well as in genetically heterogeneous mice.

Our results are in broad agreement with a series of studies over the last decade demonstrating that a prolonged inter-meal interval has major health benefits. Restricting feeding to 8–10 h per day protects mice from diet-induced obesity and insulin resistance without reducing calorie intake, perhaps by promoting regular daily rhythms in fasting and feeding[18,61]. In humans with pre-diabetes, a recent randomized clinical trial found that restricting feeding to 6 h per day improved insulin sensitivity and beta cell function without a reduction in calories or weight loss[62]. Several decades ago, one study found that the time of delivery of a once-per-day classical CR diet, or delivery of a CR diet in multiple meals limited to the dark period, had similar effects on the lifespan of mice[24]. It was recently shown that single-meal feeding of mice, resulting in an approximately 11-h fast between meals, extends lifespan and health span, although to a lesser extent than a once-per-day classical CR diet[20]. Conversely, mice fed a low-energy-density diet ad libitum spend more time eating than mice fed higher energy-density diets ad libitum, and as we also observed in the present study, have a shorter lifespan[8]. Our results, which demonstrate that prolonged daily fasting

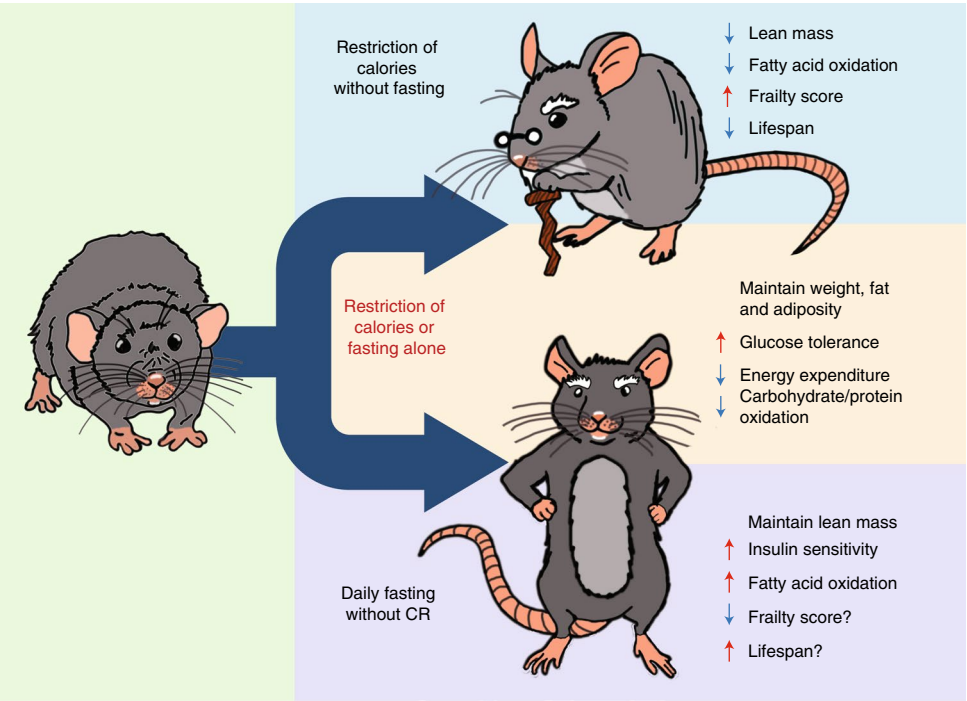

Fig. 7 | Fasting plays a critical role in the response to a CR diet. Summary figure highlighting that prolonged fasting is necessary and sufficient for many of the effects of CR.

without reduced caloric intake is sufficient to recapitulate both the metabolic impact and molecular profile of a CR diet, are in agreement with these results, and clearly demonstrate that a prolonged inter-meal interval can benefit both metabolic health and longevity.

CR extended the lifespan of non-human primates in a study conducted at the University of Wisconsin-Madison (UW)[63], but did not extend lifespan in a study conducted at the NIA[64]. Notably, NIA control animals were long-lived compared to any data on animals in captivity, possible due to the relatively low caloric intake of these animals. In both studies, when accounting for food intake and weight, animals that ate less and weighed less had increased lifespan. Other differences between the UW and NIA studies include the age at which CR was initiated and diet composition[65]. There were also differences in feeding behaviour, with animals at UW fed one main meal in the morning with a smaller snack in the afternoon[66]; as they rapidly consumed both the meal and the snack in under 1 h (personal communication, R. Colman), the animals spent the majority of the day in the fasted state. In contrast, NIA animals were fed twice a day[64]. These conditions may be comparable to the CR and MF.cr groups in our study. While there are improved biomarkers of health in humans subjected to CR[3], humans adhering to a CR diet typically eat multiple meals per day. If our findings apply to humans, sharply limiting the portion of the day during which food is consumed may maximize the health span and longevity benefits of CR, and may promote healthy ageing without requiring a reduction in calorie intake.

Time-restricted feeding studies suggest this may be case[67,68], although caution is warranted in applying these results to humans. In mice, once-per-day CR feeding performed early in the dark cycle or early in the light cycle has equivalent effects on lifespan[24]. However, in humans, skipping breakfast is associated with an increased risk of atherosclerosis and mortality[69,70]. In humans who ate one isocaloric meal per day, weight declined in the breakfast-only group, while weight increased in the dinner-only group[71]. Other studies have observed beneficial effects of once-per-day evening feeding on fat mass, but negative effects on cholesterol, blood pressure and glucose control in healthy adults[72,73], and reduced weight and blood glucose control in adults with type 2 diabetes who ate in the middle of the afternoon or later[74]. Understanding how and when we eat, and not just how much we eat, and its impact on metabolic health and longevity in humans is clearly an important area for future research.

Our work challenges long-standing assumptions about CR and, as summarized in Fig. 7, we find that collaterally imposed fasting is required for the metabolic, molecular and geroprotective effects of a CR diet. Our study has important implications for research into the mechanisms underlying the effect of CR; for example, this may explain in part why different methods of dietary restriction in worms and flies rely on different molecular pathways[55]. Re-imagining model systems to incorporate periodic fasting may provide valuable new insights into how CR works. Additionally, while restricting calories has long been viewed as unsustainable, fasting has been successfully incorporated in many fad diets and religious traditions. If these results apply to humans, fasting alone may be able to recapitulate the benefits of a CR diet without the side effects. In conclusion, our work demonstrates that daily prolonged fasting has powerful health benefits and underlies many benefits of a CR diet in mice, and that while 'you are what you eat,' it is equally true that 'you are when you eat.'

Methods

Animals, diets and feeding regimens. All procedures were performed in conformance with institutional guidelines and were approved by the Institutional Animal Care and Use Committee of the William S. Middleton Memorial Veterans Hospital (assurance ID: D16-00403). Male and female C57BL/6J and DBA/2J mice (stock nos. 000664 and 000671) were purchased from The Jackson Laboratory at 8 weeks of age and acclimatized to the animal research facility for at least 1 week before entering studies. All animals were housed in a specific pathogen-free mouse facility with a 12:12 h light–dark cycle maintained at 20–22 °C. All animals were placed on 2018 Teklad Global 18% Protein Rodent Diet for 1 week before randomization. At 10 weeks of age, mice were randomized to one of five diet groups: (1) AL, ad libitum diet; (2) CR, animals in which calories were restricted by 30%, and animals were fed once per day during the start of the light period; (3) MF.cr, animals in which calories were restricted 30%, and animals were fed three equal meals during the 12-h dark period using an automated feeder (F14

Aquarium Fish Feeder, Fish Mate)[75]; (4) Diluted AL, animals provided with ad libitum access to a low-energy diet diluted with indigestible cellulose, which reduced caloric intake by ~30%; and (5) TR.al, a feeding paradigm where mice were entrained to rapidly consume an ad libitum portion of food. Animals fed the AL, CR, MF.cr or TR.al diet were fed 2018 Teklad Global 18% Protein Rodent Diet (Envigo). Animals fed a Diluted AL diet were fed Teklad 2018 with 50% cellulose (TD.170950). A stepwise reduction in food intake by increments of 10% per week, starting at 20%, was carried out for mice in the CR group. In this study, we highlight CR regimen as a fasting model; therefore, we decided to feed these animals in the morning as it aligns best with the last feeding time point from the ad libitum-fed and MF.cr-fed animals. This feeding schedule is also widely used (for example, by the NIA aged rodent colony[23]), and the time of day at which feeding occurs has been shown not to affect the ability of CR to extend lifespan[24]. Mice in the TR.al group were entrained to eat comparably to the AL-fed group within a 3-h period during the first 2 weeks, and food was always removed 3 h after the start of feeding. Body weight and food intake were monitored weekly. Due to shredding behaviour of the Diluted AL group, we performed a comprehensive food consumption where we measured average shredded food and food left in the hopper. We found an average of 23% of the food was shredded on the bed of the cage. We accounted for this value to calculate for Diluted AL food consumption presented in this paper. CR-fed and TR.al-fed mice were fed daily at approximately 7.00. Animal rooms were maintained at 20–22 °C with 30–70% relative humidity and a 12-h light–dark cycle. The caloric intake of the mice in the AL group was calculated weekly to determine the appropriate number of calories to feed the mice in the CR and MF.cr groups. The caloric intake of the mice in the TR.al group was calculated daily to monitor food intake.

Metabolic phenotyping. Glucose and insulin tolerance tests were performed by fasting all mice overnight and then injecting either glucose (1 g per kg body weight) or insulin (0.5 U or 0.75 U per kg body weight) intraperitoneally[7]. Glucose measurements were taken using a Bayer Contour blood glucose meter and test strips. Mouse body composition was determined using an EchoMRI Body Composition Analyzer. For assay of multiple metabolic parameters (O_2, CO_2, food consumption and activity tracking), mice were acclimatized to housing in a Columbus Instruments Oxymax/CLAMS metabolic chamber system for ~24 h, and data from a continuous 24-h period were then recorded and analysed. AL-fed and Diluted AL-fed mice had ad libitum access to their respective diets; MF.cr and CR groups were fed once per day at the beginning of the light cycle as indicated in each figure.

Euthanasia and collection of tissues. Mice were euthanized in either the fasted or the fed state after 16 weeks on the diet. Mice euthanized in the fasted state were fasted overnight starting at 11.00 and then euthanized between 9.00 and 11.00 the next morning. Mice euthanized in the fed state were fed starting at 7.00 and euthanized 3 h later. Following blood collection via submandibular bleeding, mice were euthanized by cervical dislocation and tissues (liver, muscle, iWAT, epididymal WAT, brown adipose tissue and caecum) were rapidly collected, weighed and then snap frozen in liquid nitrogen.

Transcriptional profiling and analysis. RNA was extracted from liver or iWAT using TRI Reagent according to the manufacturer's protocol (Sigma-Aldrich). The concentration and purity of RNA were determined by absorbance at 260/280 nm using Nanodrop (Thermo Fisher Scientific) and sent to UW Biotechnology Center for sequencing and data annotation. Heat maps were created using Prism 8.0 with $\log_2$-transformed data. Networks were constructed using NetworkAnalyst (version 2) by protein–protein interaction[39–43] and pathways were identified with functional enrichment analysis using gene sets from KEGG.

Liver tissue metabolite extraction. *Mus musculus* liver tissue was powdered in liquid nitrogen using a mortar and pestle. Powdered tissue was transferred to an individual 1.5-ml microcentrifuge tube and incubated with 1 ml extraction solvent (80:20 ratio of methanol:H_2O at −80 °C) on dry ice for 5 min after vortexing. Tissue homogenate was centrifuged at maximum speed for 5 min at 4 °C. Supernatant was transferred to a 15-ml tube after which the remaining pellet was resuspended in 0.8 ml extraction solvent (40:40:20 ratio of acetonitrile (ACN):methanol:H_2O at −20 °C) and incubated on ice for 5 min. Tissue homogenate was again centrifuged at maximum speed for 5 min at 4 °C after which the supernatant was pooled with the previously isolated metabolite fraction. The 40:40:20 ACN:methanol:H_2O extraction was then repeated. Next, equal volumes of pooled metabolite extract for each sample was transferred to a 1.5-ml microcentrifuge tube and completely dried using a Thermo Fisher Savant ISS110 SpeedVac. Dried metabolite extracts were resuspended in 85% ACN following microcentrifugation for 5 min at maximum speed at 4 °C to pellet any remaining insoluble debris. Supernatant was then transferred to a glass vial for liquid chromatography with mass spectrometry (LC–MS) analysis.

Skeletal muscle metabolite extraction. Frozen skeletal muscle was pulverized using liquid nitrogen. Pulverized tissues (50 mg) were then homogenized in 1 ml cold (−20 °C) aqueous HPLC-grade methanol with a single 5-mm metal bead using the Qiagen TissueLyser II. Disruption was carried out at 25 Hz for 30 s. Homogenates were clarified by centrifugation, spiked with [^{13}C]succinate, and submitted to the Mass Spectrometry Facility for targeted amino acid and TCA metabolite analysis.

Targeted liquid chromatography–mass spectrometry metabolite analyses. Each prepared metabolite sample was injected onto a Thermo Fisher Scientific Vanquish UHPLC using two distinct column/buffer combinations to maximize metabolome coverage. One combination utilized a Waters XBridge BEH Amide column (100 mm × 2.1 mm, 3.5 µm) coupled to a Thermo Fisher Q-Exactive mass spectrometer. For the Waters XBridge BEH Amide column, mobile phase (A) consisted of 97% H_2O, 3% ACN, 20 mM ammonium acetate and 15 mM ammonium hydroxide (pH 9.6). Organic phase (B) consisted of 100% ACN. Metabolites were resolved using the following linear gradient: 0 min, 85% B, 0.15 ml min^{-1}; 1.5 min, 85% B, 0.15 ml min^{-1}; 5.5 min, 40% B, 0.15 ml min^{-1}; 10 min, 40% B, 0.15 ml min^{-1}; 10.5 min, 40% B, 0.3 ml min^{-1}; 14.5 min, 40% B, 0.3 ml min^{-1}; 15 min, 85% B, 0.15 ml min^{-1}; and 20 min, 85% B, 0.15 ml min^{-1}. The mass spectrometer was operated in positive ionization mode with an MS1 scan at a resolution of 70,000, an automatic gain control target of 3×10^6 and a scan range of 60–186 *m/z* and 187–900 *m/z*. The remaining combination used a Waters Acquity UPLC BEH C18 column (100 mm × 2.1 mm × 1.7 µm). For the Waters Acquity UPLC BEH C18 column, mobile phase (A) consisted of 97% H_2O, 3% methanol, 10 mM tetrabutylammonium acetate and 9 mM acetate with a final pH of 8.1–8.4. Organic phase (B) consisted of 100% methanol. Metabolites were resolved using the following linear gradient: 0 min, 95% B, 0.2 ml min^{-1}; 2.5 min, 95% B, 0.2 ml min^{-1}; 17 min, 5% B, 0.2 ml min^{-1}; 19.5 min, 5% B, 0.2 ml min^{-1}; 20 min, 95% B, 0.2 ml min^{-1}; and 25 min, 95% B, 0.2 ml min^{-1}. The mass spectrometer was operated in negative ionization mode with an MS1 scan at a resolution of 70,000, an automatic gain control target of 1×10^6 and a scan range of 85–1,275 *m/z*. Individual metabolite data were called from data files using MAVEN version 2011.6.17 (refs. [76,77]) with retention times empirically determined in-house. Top peak area values were analysed to determine metabolite expression. Heat maps were created using Spyder Anaconda 3.

Lifespan and frailty assessment. Eight-week-old male C57BL/6J mice were obtained from The Jackson Laboratory and maintained on 2018 Teklad Global (18% Protein Rodent Diet, Envigo) diet until 4 months of age. The animals were then randomized into three groups (AL, Diluted AL or CR) of equivalent body weight. Mice on the Diluted AL diet were fed a formulation of Teklad 2018 with 50% cellulose (TD.170950), resulting in an approximate 30% decrease in calorie intake. The caloric intake and of the mice in the AL group was calculated weekly to determine the appropriate number of calories to feed the mice in the CR and MF.cr groups. CR was implemented with gradual stepwise reduction in food intake by increments of 10% per week, starting at 20%, for CR mice. CR mice were fed daily at approximately 7:00. Body weight and food intake were monitored every week until food intake was stabilized and then monitored every other week. Mice were housed in a specific pathogen-free mouse facility with a 12:12 h light–dark cycle maintained at 20–22 °C. Mice were euthanized for humane reasons if moribund, if the mice developed other specified problems (for example, excessive tumour burden) or following the recommendation of the facility veterinarian. Mice that developed rectal prolapse were treated with Anusol Plus daily; mice euthanized due to rectal prolapse without other health abnormalities were censored as of the date of euthanasia. Mice were censored as of the date of death if death was associated with a procedure.

Frailty was assessed using a 25-item frailty index based on the procedures defined by Whitehead et al.[78]. The items scored included alopecia, loss of fur colour, dermatitis, loss of whiskers, coat condition, tumours, distended abdomen, kyphosis, tail stiffening, gait disorders, tremor, body condition score, vestibular disturbance, cataracts, corneal opacity, eye discharge/swelling, microphthalmia, nasal discharge, malocclusions, rectal prolapse, vaginal/uterine/penile prolapse, diarrheoa, breathing rate/depth, mouse grimace score and piloerection.

Bomb calorimetry. We determined the caloric content of diet and faeces of 19-month-old C57BL/6J male mice (diet implementation at 4 months) with an adiabatic bomb calorimeter (6200ea Oxygen Bomb Calorimeter; Parr Instrument Company). Bombs were calibrated using benzoic acid before use.

Intestinal barrier integrity. Twenty-month-old C57BL/6J mice (diet implementation at 4 months) were fasted from food for 4 h before and from both food and water 4 h after an oral gavage of 200 µl (50 mg ml^{-1}) FITC-dextran (4 kDa; Sigma-Aldrich). Blood was collected at 0, 30, 60, 120 and 240 min and fluorescence intensity was measured using an excitation wavelength of 493 nm and an emission wavelength of 517 nm.

Radar charts. Values for radar charts were calculated from the percentage change from AL within the specific strain and sex. The distance from the centre represents the effect of each restricted diet versus AL-fed mice (no difference = 100%). Data are presented as the average of diet group per sex for each strain.

Statistics. Data are presented as the mean ± s.e.m. unless otherwise specified. For the box plots, the centre line represents the median, box limits indicate the upper and lower 25th to 75th percentiles and whiskers extend to the smallest and largest

data values. Analyses were performed using Excel (2010 and 2016, Microsoft) or Prism 8 (GraphPad Software). Statistical analyses were performed using one-way or two-way ANOVA followed by Tukey–Kramer post hoc test, as specified in the figure legends. Other statistical details are available in the figure legends. In all figures, *n* represents the number of biologically independent animals. Sample sizes for longevity studies were determined in consultation with previously published power tables[79]. Sample sizes for metabolic studies were determined based on our previously published experimental results with the effects of dietary interventions[9], with the goal of having >90% power to detect a change in AUC during a glucose tolerance test ($P < 0.05$). Data distribution was assumed to be normal, but this was not formally tested. Sample sizes for molecular analyses were chosen in consultation with core facility staff and experienced laboratory personnel.

Blinding. Investigators were blinded to diet groups during data collection whenever feasible, but this was not usually possible or feasible as cages were clearly marked to indicate the diet provided, and the size and body composition of the mice was altered by strain and diet. However, blinding is not relevant to the majority of the studies conducted here, as the data are collected in numeric form, which is not readily subject to bias due to the need for subjective interpretation. Investigators were not blinded during necropsies, as the size and body composition of the mice was altered by strain and diet and group identity was therefore readily apparent.

Randomization. All studies were performed on animals or on tissues collected from animals. Animals of each sex and strain were randomized into groups of equivalent weight before the beginning of the in vivo studies.

Reporting Summary. Further information on research design is available in the Nature Research Reporting Summary linked to this article.

Data availability

RNA-sequencing data have been deposited with the Gene Expression Omnibus and are available under accession number GSE168262. Source data are provided with this paper. Other data that support the plots and findings of this study are available from the corresponding author upon reasonable request.

Received: 24 February 2021; Accepted: 30 August 2021;
Published online: 18 October 2021

References

1. Green, C. L., Lamming, D. W. & Fontana, L. Molecular mechanisms of dietary restriction promoting health and longevity. *Nat. Rev. Mol. Cell Biol.* https://doi.org/10.1038/s41580-021-00411-4 (2021).
2. Colman, R. J. et al. Caloric restriction reduces age-related and all-cause mortality in rhesus monkeys. *Nat. Commun.* **5**, 3557 (2014).
3. Kraus, W. E. et al. 2 years of calorie restriction and cardiometabolic risk (CALERIE): exploratory outcomes of a multicentre, phase 2, randomised controlled trial. *Lancet Diabetes Endocrinol.* **7**, 673–683 (2019).
4. Belsky, D. W., Huffman, K. M., Pieper, C. F., Shalev, I. & Kraus, W. E. Change in the rate of biological aging in response to caloric restriction: CALERIE Biobank analysis. *J. Gerontol. A Biol. Sci. Med. Sci.* **73**, 4–10 (2017).
5. Das, S. K. et al. Body-composition changes in the comprehensive assessment of long-term effects of reducing intake of energy (CALERIE)-2 study: a 2-year randomized controlled trial of calorie restriction in nonobese humans. *Am. J. Clin. Nutr.* **105**, 913–927 (2017).
6. Balasubramanian, P., Howell, P. R. & Anderson, R. M. Aging and caloric restriction research: a biological perspective with translational potential. *EBioMedicine* **21**, 37–44 (2017).
7. Yu, D. et al. Calorie-restriction-induced insulin sensitivity is mediated by adipose mTORC2 and not required for lifespan extension. *Cell Rep.* **29**, 236–248 (2019).
8. Solon-Biet, S. M. et al. The ratio of macronutrients, not caloric intake, dictates cardiometabolic health, aging and longevity in ad libitum-fed mice. *Cell Metab.* **19**, 418–430 (2014).
9. Fontana, L. et al. Decreased consumption of branched-chain amino acids improves metabolic health. *Cell Rep.* **16**, 520–530 (2016).
10. Grandison, R. C., Piper, M. D. & Partridge, L. Amino-acid imbalance explains extension of lifespan by dietary restriction in *Drosophila*. *Nature* **462**, 1061–1064 (2009).
11. Lu, J. et al. Sestrin is a key regulator of stem cell function and lifespan in response to dietary amino acids. *Nat. Aging* **1**, 60–72 (2021).
12. Solon-Biet, S. M. et al. Branched chain amino acids impact health and lifespan indirectly via amino acid balance and appetite control. *Nat. Metab.* **1**, 532–545 (2019).
13. Yoshida, S. et al. Role of dietary amino acid balance in diet restriction-mediated lifespan extension, renoprotection, and muscle weakness in aged mice. *Aging Cell* **17**, e12796 (2018).
14. Speakman, J. R., Mitchell, S. E. & Mazidi, M. Calories or protein? The effect of dietary restriction on lifespan in rodents is explained by calories alone. *Exp. Gerontol.* **86**, 28–38 (2016).
15. Acosta-Rodriguez, V. A., de Groot, M. H. M., Rijo-Ferreira, F., Green, C. B. & Takahashi, J. S. Mice under caloric restriction self-impose a temporal restriction of food intake as revealed by an automated feeder system. *Cell Metab.* **26**, 267–277 (2017).
16. Bruss, M. D., Khambatta, C. F., Ruby, M. A., Aggarwal, I. & Hellerstein, M. K. Calorie restriction increases fatty acid synthesis and whole body fat oxidation rates. *Am. J. Physiol. Endocrinol. Metab.* **298**, E108–E116 (2010).
17. Longo, V. D. & Mattson, M. P. Fasting: molecular mechanisms and clinical applications. *Cell Metab.* **19**, 181–192 (2014).
18. Hatori, M. et al. Time-restricted feeding without reducing caloric intake prevents metabolic diseases in mice fed a high-fat diet. *Cell Metab.* **15**, 848–860 (2012).
19. Chaix, A., Zarrinpar, A., Miu, P. & Panda, S. Time-restricted feeding is a preventative and therapeutic intervention against diverse nutritional challenges. *Cell Metab.* **20**, 991–1005 (2014).
20. Mitchell, S. J. et al. Daily fasting improves health and survival in male mice independent of diet composition and calories. *Cell Metab.* **29**, 221–228 (2019).
21. Mitchell, S. J. et al. Effects of sex, strain, and energy intake on hallmarks of aging in mice. *Cell Metab.* **23**, 1093–1112 (2016).
22. Liao, C. Y., Rikke, B. A., Johnson, T. E., Diaz, V. & Nelson, J. F. Genetic variation in the murine lifespan response to dietary restriction: from life extension to life shortening. *Aging Cell* **9**, 92–95 (2010).
23. Turturro, A. et al. Growth curves and survival characteristics of the animals used in the biomarkers of aging program. *J. Gerontol. A Biol. Sci. Med. Sci.* **54**, B492–B501 (1999).
24. Nelson, W. & Halberg, F. Meal-timing, circadian rhythms and life span of mice. *J. Nutr.* **116**, 2244–2253 (1986).
25. Fernandes, G., Yunis, E. J. & Good, R. A. Influence of diet on survival of mice. *Proc. Natl Acad. Sci. USA* **73**, 1279–1283 (1976).
26. Hempenstall, S., Picchio, L., Mitchell, S. E., Speakman, J. R. & Selman, C. The impact of acute caloric restriction on the metabolic phenotype in male C57BL/6 and DBA/2 mice. *Mech. Ageing Dev.* **131**, 111–118 (2010).
27. Hasek, B. E. et al. Dietary methionine restriction enhances metabolic flexibility and increases uncoupled respiration in both fed and fasted states. *Am. J. Physiol. Regul. Integr. Comp. Physiol.* **299**, R728–R739 (2010).
28. Abreu-Vieira, G., Xiao, C., Gavrilova, O. & Reitman, M. L. Integration of body temperature into the analysis of energy expenditure in the mouse. *Mol. Metab.* **4**, 461–470 (2015).
29. Haws, S. A., Leech, C. M. & Denu, J. M. Metabolism and the epigenome: a dynamic relationship. *Trends Biochem. Sci.* https://doi.org/10.1016/j.tibs.2020.04.002 (2020).
30. Haws, S. A. et al. Methyl-metabolite depletion elicits adaptive responses to support heterochromatin stability and epigenetic persistence. *Mol. Cell* **78**, 210–223(2020).
31. Leatham-Jensen, M. et al. Lysine 27 of replication-independent histone H3.3 is required for Polycomb target gene silencing but not for gene activation. *PLoS Genet.* **15**, e1007932 (2019).
32. Meyer, C., Dostou, J. M., Welle, S. L. & Gerich, J. E. Role of human liver, kidney, and skeletal muscle in postprandial glucose homeostasis. *Am. J. Physiol. Endocrinol. Metab.* **282**, E419–E427 (2002).
33. Wolfe, R. R. The underappreciated role of muscle in health and disease. *Am. J. Clin. Nutr.* **84**, 475–482 (2006).
34. Rhoads, T. W. et al. Molecular and functional networks linked to sarcopenia prevention by caloric restriction in rhesus monkeys. *Cell Syst.* **10**, 156–168 (2020).
35. McKiernan, S. H. et al. Caloric restriction delays aging-induced cellular phenotypes in rhesus monkey skeletal muscle. *Exp. Gerontol.* **46**, 23–29 (2011).
36. Pugh, T. D. et al. A shift in energy metabolism anticipates the onset of sarcopenia in rhesus monkeys. *Aging Cell* **12**, 672–681 (2013).
37. Chang, J. et al. Effect of aging and caloric restriction on the mitochondrial proteome. *J. Gerontol. A Biol. Sci. Med. Sci.* **62**, 223–234 (2007).
38. Parks, B. W. et al. Genetic architecture of insulin resistance in the mouse. *Cell Metab.* **21**, 334–347 (2015).
39. Xia, J., Benner, M. J. & Hancock, R. E. NetworkAnalyst–integrative approaches for protein–protein interaction network analysis and visual exploration. *Nucleic Acids Res.* **42**, W167–W174 (2014).
40. Xia, J. et al. INMEX–a web-based tool for integrative meta-analysis of expression data. *Nucleic Acids Res.* **41**, W63–W70 (2013).
41. Xia, J., Gill, E. E. & Hancock, R. E. NetworkAnalyst for statistical, visual and network-based meta-analysis of gene expression data. *Nat. Protoc.* **10**, 823–844 (2015).
42. Xia, J., Lyle, N. H., Mayer, M. L., Pena, O. M. & Hancock, R. E. INVEX–a web-based tool for integrative visualization of expression data. *Bioinformatics* **29**, 3232–3234 (2013).

43. Zhou, G. et al. NetworkAnalyst 3.0: a visual analytics platform for comprehensive gene expression profiling and meta-analysis. *Nucleic Acids Res.* **47**, W234–W241 (2019).
44. Kane, A. E. et al. Impact of longevity interventions on a validated mouse clinical frailty index. *J. Gerontol. A Biol. Sci. Med. Sci.* **71**, 333–339 (2016).
45. Bellantuono, I. et al. A toolbox for the longitudinal assessment of health span in aging mice. *Nat. Protoc.* **15**, 540–574 (2020).
46. Aon, M. A. et al. Untangling determinants of enhanced health and lifespan through a multi-omics approach in mice. *Cell Metab.* **32**, 100–116 (2020).
47. Duffy, P. H. et al. Effect of chronic caloric restriction on physiological variables related to energy metabolism in the male Fischer 344 rat. *Mech. Ageing Dev.* **48**, 117–133 (1989).
48. Masoro, E. J., McCarter, R. J., Katz, M. S. & McMahan, C. A. Dietary restriction alters characteristics of glucose fuel use. *J. Gerontol.* **47**, B202–B208 (1992).
49. Green, C. L. et al. The effects of graded levels of calorie restriction: IX. Global metabolomic screen reveals modulation of carnitines, sphingolipids and bile acids in the liver of C57BL/6 mice. *Aging Cell* **16**, 529–540 (2017).
50. Green, C. L. et al. The effects of graded levels of calorie restriction: XIV. Global metabolomics screen reveals brown adipose tissue changes in amino acids, catecholamines, and antioxidants after short-term restriction in C57BL/6 mice. *J. Gerontol. A Biol. Sci. Med. Sci.* **75**, 218–229 (2020).
51. Green, C. L. et al. The effects of graded levels of calorie restriction: XIII. Global metabolomics screen reveals graded changes in circulating amino acids, vitamins, and bile acids in the plasma of C57BL/6 mice. *J. Gerontol. A Biol. Sci. Med. Sci.* **74**, 16–26 (2019).
52. Green, C. L. et al. The effects of graded levels of calorie restriction: XVI. Metabolomic changes in the cerebellum indicate activation of hypothalamocerebellar connections driven by hunger responses. *J. Gerontol. A Biol. Sci. Med. Sci.* **76**, 601–610 (2021).
53. Kokkonen, G. C. & Barrows, C. H. The effect of dietary cellulose on life span and biochemical variables of male mice. *Age* **11**, 7–9 (1988).
54. Mair, W., Piper, M. D. & Partridge, L. Calories do not explain extension of life span by dietary restriction in *Drosophila*. *PLoS Biol.* **3**, e223 (2005).
55. Greer, E. L. & Brunet, A. Different dietary restriction regimens extend lifespan by both independent and overlapping genetic pathways in *C. elegans*. *Aging Cell* **8**, 113–127 (2009).
56. Lyn, J. C., Naikkhwah, W., Aksenov, V. & Rollo, C. D. Influence of two methods of dietary restriction on life history features and aging of the cricket *Acheta domesticus*. *Age* **33**, 509–522 (2011).
57. Derous, D. et al. The effects of graded levels of calorie restriction: X. Transcriptomic responses of epididymal adipose tissue. *J. Gerontol. A Biol. Sci. Med. Sci.* **73**, 279–288 (2017).
58. Derous, D. et al. The effects of graded levels of calorie restriction: XI. Evaluation of the main hypotheses underpinning the life extension effects of CR using the hepatic transcriptome. *Aging* **9**, 1770–1824 (2017).
59. Froy, O. & Miskin, R. Effect of feeding regimens on circadian rhythms: implications for aging and longevity. *Aging* **2**, 7–27 (2010).
60. Barrington, W. T. et al. Improving metabolic health through precision dietetics in mice. *Genetics* **208**, 399–417 (2018).
61. Chaix, A., Lin, T., Le, H. D., Chang, M. W. & Panda, S. Time-restricted feeding prevents obesity and metabolic syndrome in mice lacking a circadian clock. *Cell Metab.* **29**, 303–319 (2019).
62. Sutton, E. F. et al. Early time-restricted feeding improves insulin sensitivity, bood pressure, and oxidative stress even without weight loss in men with prediabetes. *Cell Metab.* **27**, 1212–1221 (2018).
63. Colman, R. J. et al. Caloric restriction delays disease onset and mortality in rhesus monkeys. *Science* **325**, 201–204 (2009).
64. Mattison, J. A. et al. Impact of caloric restriction on health and survival in rhesus monkeys from the NIA study. *Nature* **489**, 318–321 (2012).
65. Mattison, J. A. et al. Caloric restriction improves health and survival of rhesus monkeys. *Nat. Commun.* **8**, 14063 (2017).
66. Ramsey, J. J. et al. Dietary restriction and aging in rhesus monkeys: the University of Wisconsin study. *Exp. Gerontol.* **35**, 1131–1149 (2000).
67. Cienfuegos, S. et al. Effects of 4-h and 6-h time-restricted feeding on weight and cardiometabolic health: a randomized controlled trial in adults with obesity. *Cell Metab.* **32**, 366–378 (2020).
68. Wilkinson, M. J. et al. Ten-hour time-restricted eating reduces weight, blood pressure, and atherogenic lipids in patients with metabolic syndrome. *Cell Metab.* **31**, 92–104 (2020).
69. Yokoyama, Y. et al. Erratum for Yokoyama et al., 'skipping breakfast and risk of mortality from cancer, circulatory diseases and all causes: findings from the Japan Collaborative Cohort Study'. *Yonago Acta Med.* **62**, 308 (2019).
70. Uzhova, I. et al. The importance of breakfast in atherosclerosis disease: insights from the PESA Study. *J. Am. Coll. Cardiol.* **70**, 1833–1842 (2017).
71. Cornelissen, G. When you eat matters: 60 years of Franz Halberg's nutrition chronomics. *Open Nutraceuticals J.* **5**, 16–44 (2012).
72. Stote, K. S. et al. A controlled trial of reduced meal frequency without caloric restriction in healthy, normal-weight, middle-aged adults. *Am. J. Clin. Nutr.* **85**, 981–988 (2007).
73. Carlson, O. et al. Impact of reduced meal frequency without caloric restriction on glucose regulation in healthy, normal-weight middle-aged men and women. *Metabolism* **56**, 1729–1734 (2007).
74. Arnason, T. G., Bowen, M. W. & Mansell, K. D. Effects of intermittent fasting on health markers in those with type 2 diabetes: a pilot study. *World J. Diabetes* **8**, 154–164 (2017).
75. Dommerholt, M. B., Dionne, D. A., Hutchinson, D. F., Kruit, J. K. & Johnson, J. D. Metabolic effects of short-term caloric restriction in mice with reduced insulin gene dosage. *J. Endocrinol.* **237**, 59–71 (2018).
76. Clasquin, M. F., Melamud, E. & Rabinowitz, J. D. LC-MS data processing with MAVEN: a metabolomic analysis and visualization engine. *Curr. Protoc. Bioinformatics* https://doi.org/10.1002/0471250953.bi1411s37 (2012).
77. Melamud, E., Vastag, L. & Rabinowitz, J. D. Metabolomic analysis and visualization engine for LC-MS data. *Anal. Chem.* https://doi.org/10.1021/ac1021166 (2010).
78. Whitehead, J. C. et al. A clinical frailty index in aging mice: comparisons with frailty index data in humans. *J. Gerontol. A Biol. Sci. Med. Sci.* **69**, 621–632 (2014).
79. Liang, H. et al. Genetic mouse models of extended lifespan. *Exp. Gerontol.* **38**, 1353–1364 (2003).

Acknowledgements

We thank all members of the laboratory of D.W.L., as well as J. Simcox and R. Jain, for their valuable insights and comments. We thank S. Simpson and S. Solon-Biet for advice regarding animal care. We thank T. Herfel (Envigo) for assistance with the formulation of the Diluted AL diet. We thank M. Schaid for critical reading of the manuscript. The laboratory of D.W.L. is supported in part by the National Institutes of Health (NIH)/NIA (AG050135, AG051974, AG056771, AG062328 and AG061635 to D.W.L.), NIH/National Institute of Diabetes and Digestive and Kidney Diseases (DK125859 to D.W.L and J.M.D.) and start-up funds from the UW School of Medicine and Public Health and Department of Medicine (to D.W.L.). Metabolomic and histone proteomic analysis was supported in part by a grant from the NIH (R37GM059785 to J.M.D.) and a UAB Nathan Shock Center of Excellence in the Basic Biology of Aging (P30AG050886) Core Services Pilot Award (to D.W.L.). Bomb calorimetry was supported by S10OD028739 (to C.-L.E.Y.), and gut integrity analysis was supported in part by DK124696 (to C.-L.E.Y.). H.H.P. is supported in part by a NIA F31 pre-doctoral fellowship (AG066311). C.L.G. is supported by a Glenn Foundation for Medical Research Postdoctoral Fellowship and was supported in part by a generous gift from D. Philanthropies. N.E.R. was supported in part by a training grant from the UW Institute on Aging (NIA T32 AG000213). S.A.H. was supported in part by a training grant from the UW Metabolism and Nutrition Training Program (T32 DK007665). Support for this research was provided by the UW Office of the Vice Chancellor for Research and Graduate Education with funding from the Wisconsin Alumni Research Foundation. This work was supported in part by the US Department of Veterans Affairs (I01-BX004031), and this work was supported using facilities and resources from the William S. Middleton Memorial Veterans Hospital. The content is solely the responsibility of the authors and does not necessarily represent the official views of the NIH. This work does not represent the views of the Department of Veterans Affairs or the US Government.

Author contributions

Experiments were performed in the laboratories of D.W.L., J.M.D. and C.-L.E.Y. at UW-Madison and in the UAB Nathan Shock Center Mitometabolism Core. All authors participated in the performance of the experiments and/or analysed the data. H.H.P., S.A.H., J.Z., J.M.D. and D.W.L. prepared the manuscript.

Competing interests

D.W.L. has received funding from, and is a scientific advisory board member of, Aeovian Pharmaceuticals, which seeks to develop novel, selective mTOR inhibitors for the treatment of various diseases. J.M.D. is a consultant for FORGE Life Sciences and co-founder of Galilei Bio-Sciences. The remaining authors declare no competing interests.

Additional information

Extended data is available for this paper at https://doi.org/10.1038/s42255-021-00466-9.

Supplementary information The online version contains supplementary material available at https://doi.org/10.1038/s42255-021-00466-9.

Correspondence and requests for materials should be addressed to Dudley W. Lamming.

Peer review information *Nature Metabolism* thanks Leonie Heilbronn and the other, anonymous, reviewer(s) for their contribution to the peer review of this work. Primary Handling Editor: Christoph Schmitt.

Reprints and permissions information is available at www.nature.com/reprints.

Publisher's note Springer Nature remains neutral with regard to jurisdictional claims in published maps and institutional affiliations.

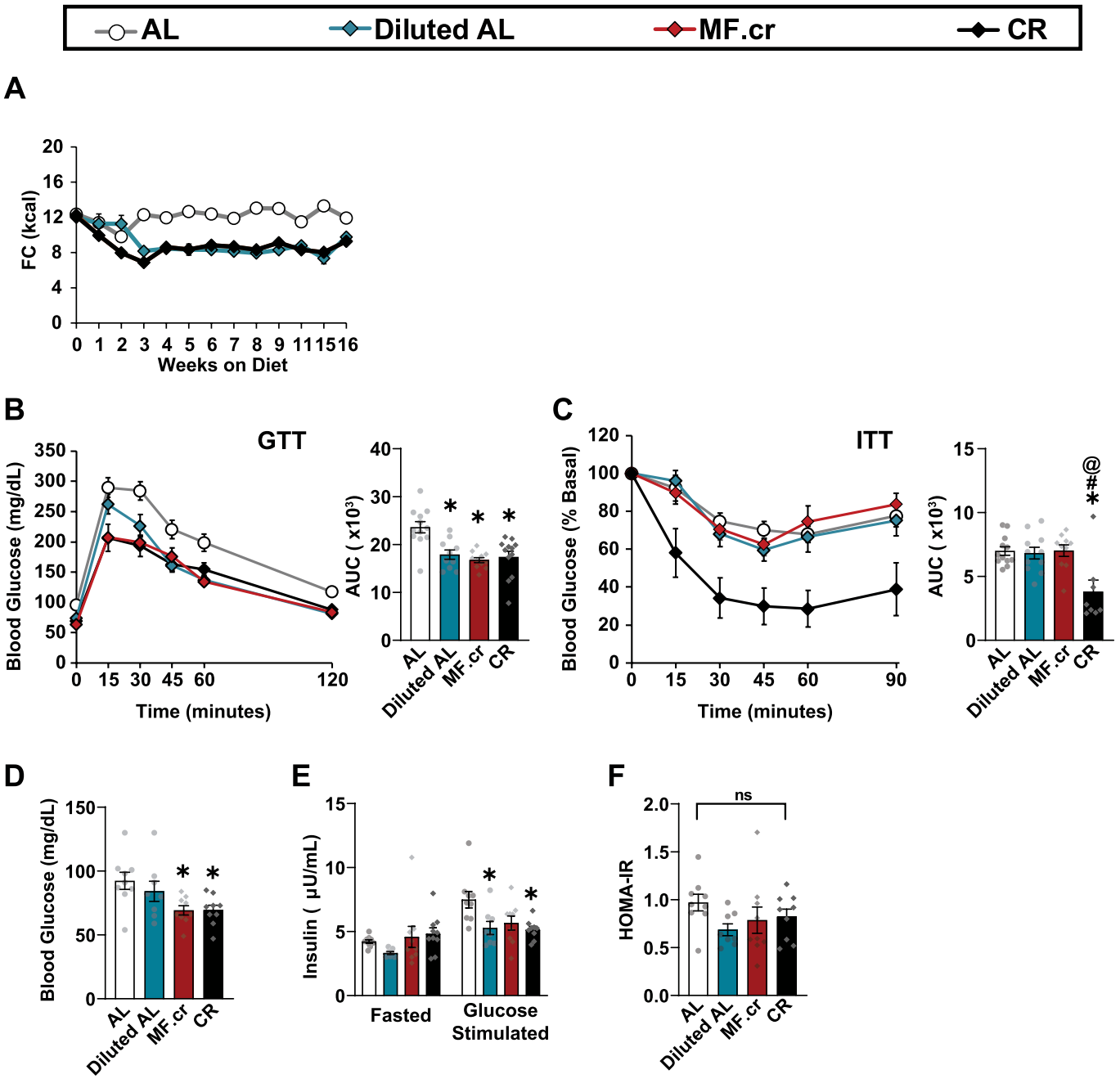

Extended Data Fig. 1 | Additional measures of glucose homeostasis in male C57BL/6J mice. (**a**) Food Consumption (**b**) Glucose (AL, n = 12; Diluted AL, n = 10; MF.cr, n = 11; CR, n = 12 biologically independent mice) (**c**) and insulin (AL, n = 12; Diluted AL, n = 11; MF.cr, n = 10; CR, n = 8 biologically independent mice) tolerance tests after 13 or 14 weeks on the indicated diets. * symbol represents a significant difference versus AL-fed mice (p = 0.0009); # symbol represents a significant difference versus Diluted AL-fed mice (p = 0.0021); * symbol represents a significant difference versus MF.cr-fed mice (p = 0.0013) based on Tukey's test post one-way ANOVA. (D-F) Fasting blood glucose (**d**), fasting and glucose-stimulated insulin secretion (15 minutes) (**e**), and calculated HOMA-IR (F). (**d-f**) AL, n = 9; Diluted AL, n = 8; MF.cr, n = 9; CR, n = 9 biologically independent mice; * symbol represents a significant difference versus AL-fed mice (Diluted AL, p = 0.0256; CR, p = 0.0127); insulin levels in fasted and glucose-stimulated states were analyzed separately. All data are represented as mean ± SEM.

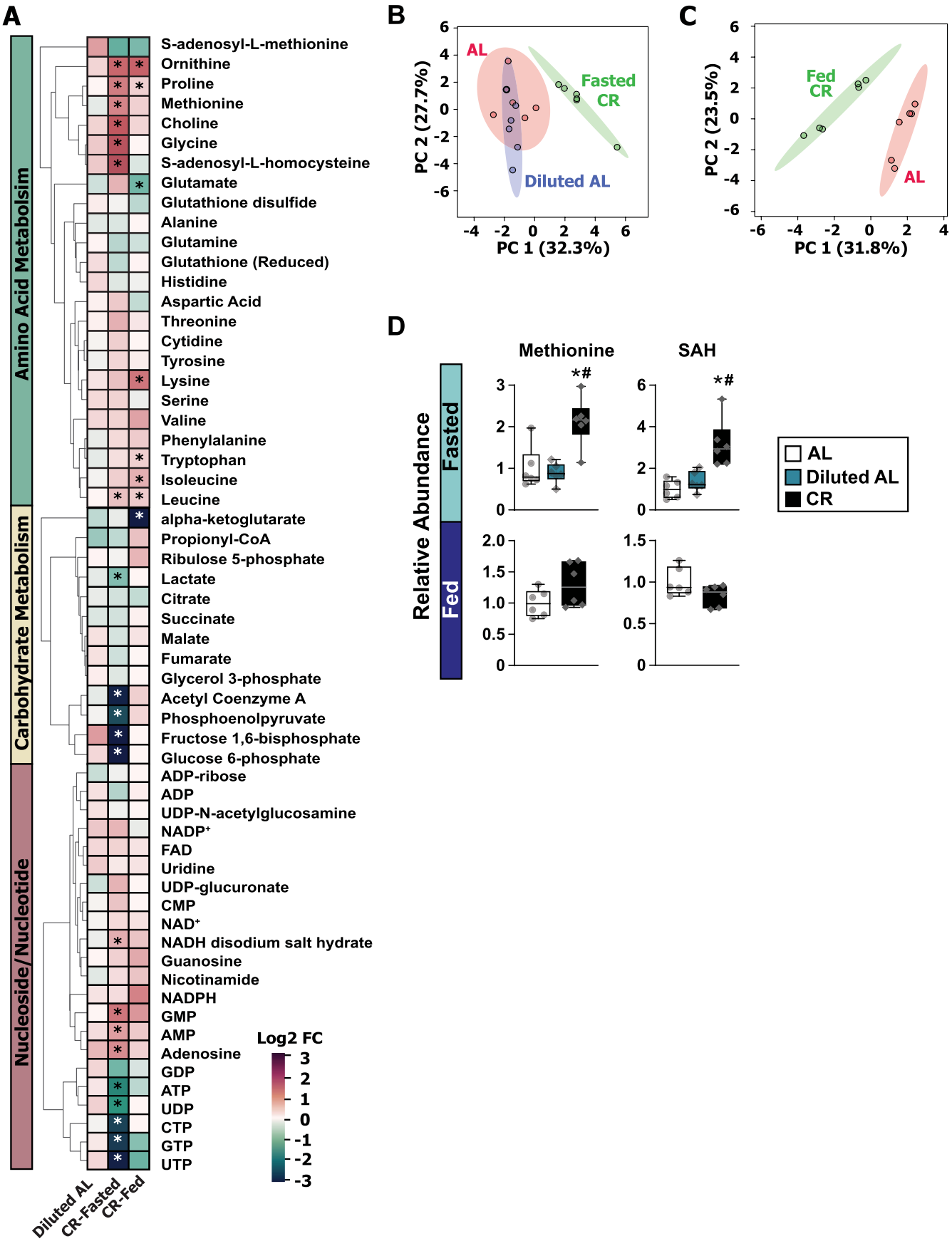

Extended Data Fig. 2 | See next page for caption.

Extended Data Fig. 2 | Fasting is required for CR-mediated reprogramming of the hepatic metabolome. Targeted metabolomics were performed on the livers of male C57BL/6J mice fed AL, Diluted AL and CR diets (n = 6 biologically independent mice per diet). **a**) Heatmap of 59 targeted metabolites, represented as log_2-fold change vs. AL-fed mice. **b**) sPLS-DA of liver metabolomics with CR mice sacrificed in the fasted state. **c**) sPLS-DA of liver metabolomics with CR sacrificed in the fed state. (**d**) Relative abundance of methionine and its metabolite S-Adenosyl-Homocysteine. * symbol represents a significant difference versus AL mice ($p \leq 0.0023$); # symbol represents a significant difference versus Diluted AL mice ($p \leq 0.0024$) based on Tukey's test post one-way ANOVA. Overlaid box plots show center as median and 25^{th}-75^{th} percentiles; whiskers represent minima and maxima.

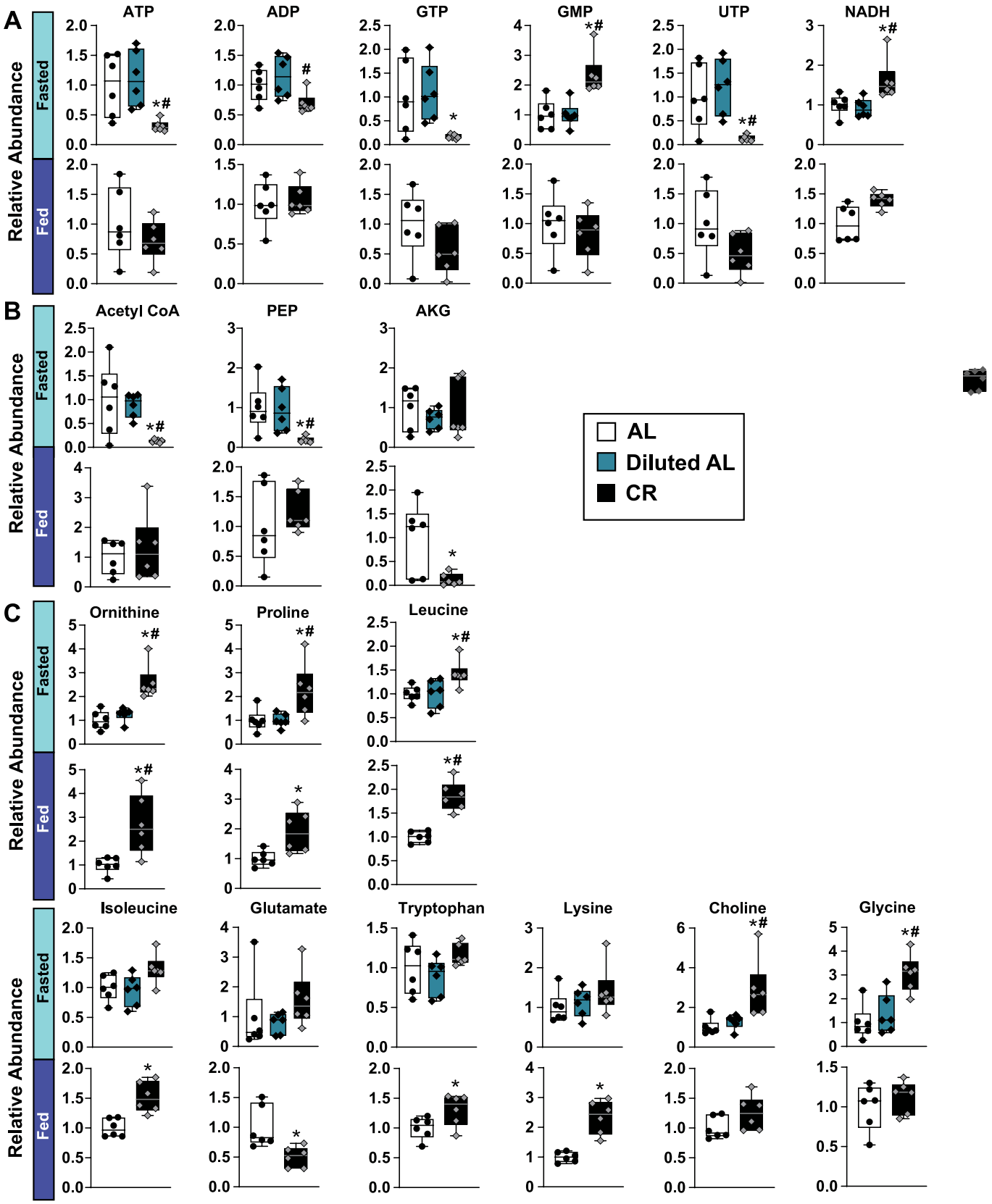

Extended Data Fig. 3 | Additional hepatic metabolomic data. (**a-c**) Hepatic metabolites that showed a statistically significant difference during the fasted or fed state (n = 6 biologically independent mice per diet). **a**) Relative abundance of nucleotide/nucleoside metabolites. **b**) Relative abundance of TCA cycle metabolites. **c**) Relative abundance of amino acid metabolites. (**a-c**) * symbol represents a significant difference versus AL mice ($p \leq 0.05$); # symbol represents a significant difference versus Diluted AL mice ($p \leq 0.05$) based on Tukey's test post one-way ANOVA. Overlaid box plots show center as median and 25th-75th percentiles; whiskers represent minima and maxima.

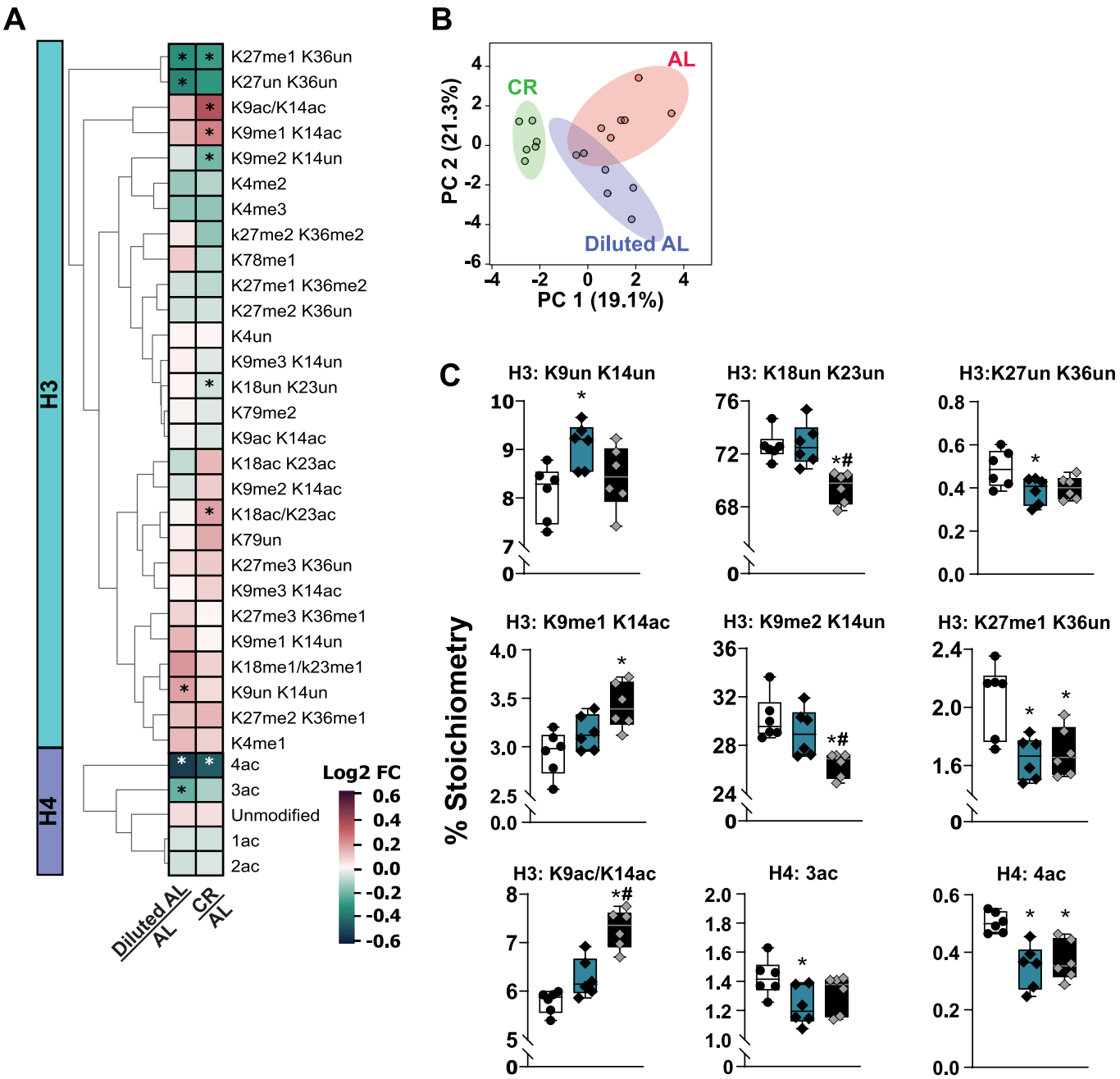

Extended Data Fig. 4 | Fasting is required for CR-mediated reprogramming of the hepatic epigenome. Histone proteomics were performed on the livers of male C57BL/6J mice fed AL, Diluted AL and CR diets (n = 6 mice per group). **a**) Heatmap of histone H3 and H4 peptides represented as log2-fold change from AL. B) sPLS-DA of histone modifications. **c**) Statistically significant modified histones. (**a-c**) * symbol represents a significant difference versus AL mice ($p \leq 0.05$); # symbol represents a significant difference versus Diluted AL mice ($p \leq 0.05$) based on Tukey's test post one-way ANOVA. Overlaid box plots show center as median and 25th-75th percentiles; whiskers represent minima and maxima.

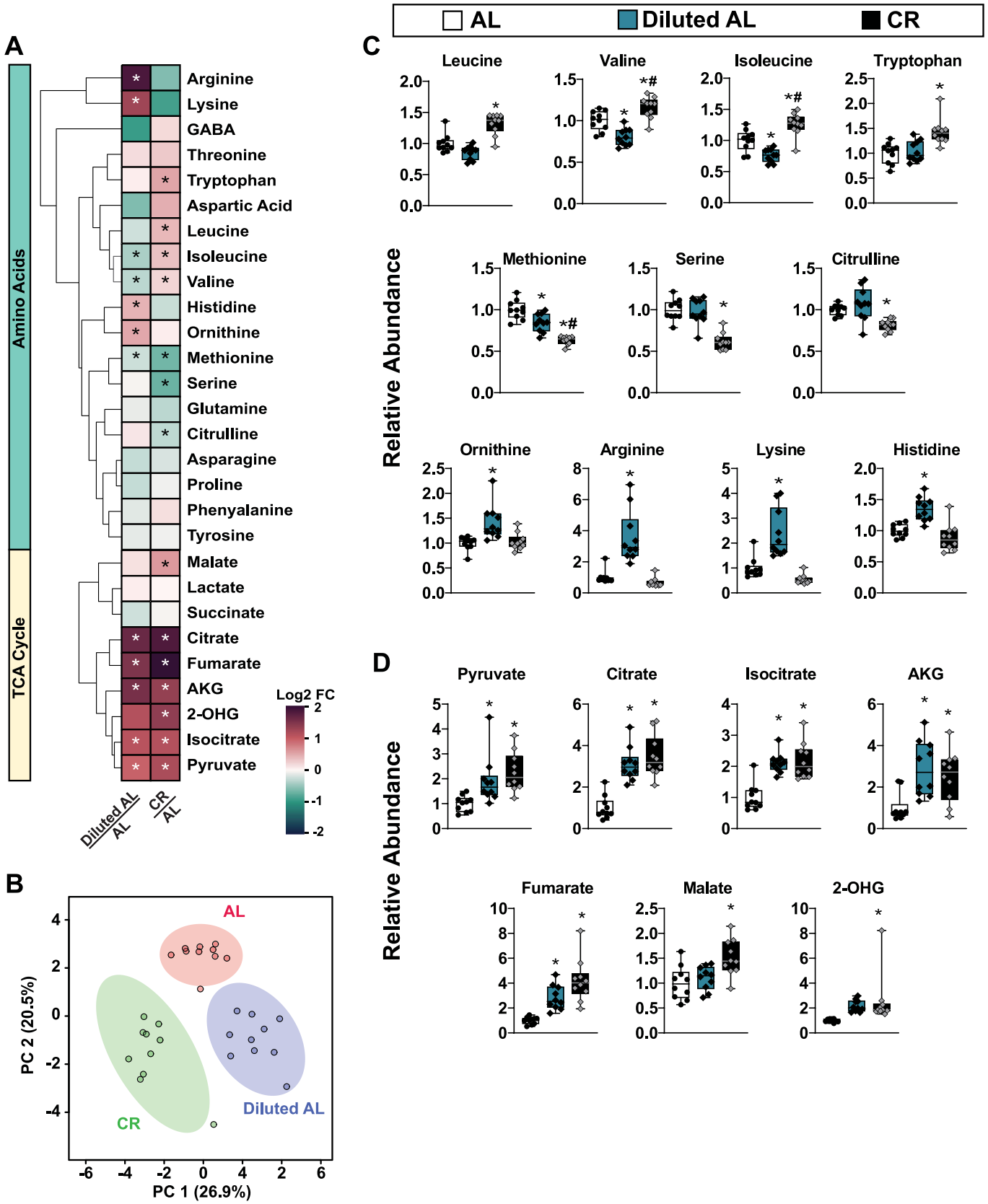

Extended Data Fig. 5 | See next page for caption.

Extended Data Fig. 5 | Metabolomic profile of skeletal muscle from AL, Diluted AL and CR mice. Targeted metabolomics were performed on skeletal muscle from male C57BL/6J mice fed AL, Diluted AL, and CR diets (n = 10 biologically independent mice per diet). **a**) Heatmap of 28 targeted metabolites, represented as log2-fold change vs. AL-fed mice. **b**) sPLS-DA of skeletal muscle metabolites. **c**) Relative abundance of amino acid metabolites. **d**) Relative abundance of TCA cycle metabolites. (**a–d**) * symbol represents a significant difference versus AL mice ($p \leq 0.05$); # symbol represents a significant difference versus Diluted AL mice ($p \leq 0.05$) based on Tukey's test post one-way ANOVA. Overlaid box plots show center as median and 25th-75th percentiles; whiskers represent minima and maxima.

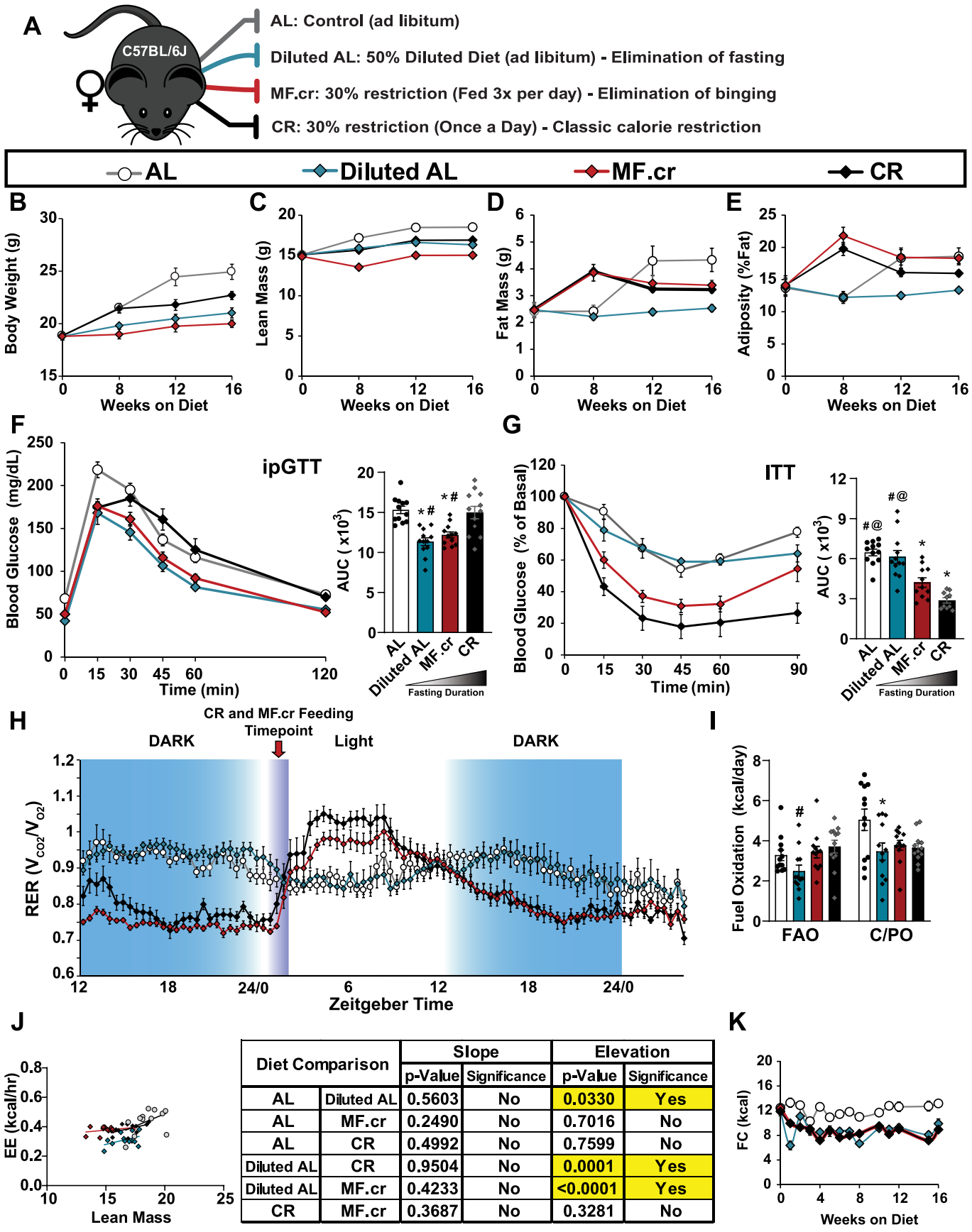

Diet Comparison		Slope		Elevation	
		p-Value	Significance	p-Value	Significance
AL	Diluted AL	0.5603	No	0.0330	Yes
AL	MF.cr	0.2490	No	0.7016	No
AL	CR	0.4992	No	0.7599	No
Diluted AL	CR	0.9504	No	0.0001	Yes
Diluted AL	MF.cr	0.4233	No	<0.0001	Yes
CR	MF.cr	0.3687	No	0.3281	No

Extended Data Fig. 6 | See next page for caption.

Extended Data Fig. 6 | The effect of three calorie restriction regimens on female C57BL/6J mice. (**a**) Outline of feeding regimens: AL, Diluted AL, CR and MF.cr. (**b-e**) Body composition measurement over 16 weeks on diet (AL, n = 12; Diluted AL, n = 10; MF.cr, n = 12; CR, n = 12 biologically independent mice); total body weight (**b**), lean mass (**c**), fat mass (**d**) and adiposity (**e**). (**f-g**) Glucose (n = 12 biologically independent mice per diet) (**f**) and insulin (AL, n = 12; Diluted AL, n = 12; MF.cr, n = 11; CR, n = 10 biologically independent mice) (**g**) tolerance tests after 9 or 10 weeks on the indicated diets. * symbol represents a significant difference versus AL-fed mice (Diluted AL, $p < 0.0001$; MF.cr, $p \leq 0.0012$, CR, $p < 0.0001$); # symbol represents a significant difference versus Diluted AL-fed mice (MF.cr, $p = 0.0019$; CR, $p \leq 0.0001$); @ symbol represents a significant difference versus MF.cr-fed mice (CR, $p = 0.0043$) based on Tukey's test post one-way ANOVA. (**h-j**) Metabolic chamber analysis of mice fed the indicated diets. (**h**) Respiratory exchange ratio vs. time (n = 12 biologically independent mice per diet) (**i**) Fuel utilization was calculated for the 24-hour period following the indicated (arrow) refeeding time (n = 12 biologically independent mice per diet). * symbol represents a significant difference versus AL (Diluted AL, $p = 0.0255$); # symbol represents a significant difference versus Diluted AL (CR, $p = 0.0274$) based on Tukey's test post one-way ANOVA performed separately for FAO and C/PO). (**j**) Energy expenditure as a function of lean mass was calculated for the 24-hour period following the indicated (arrow) refeeding time (n = 12 biologically independent mice per diet, data for each individual mouse is plotted; slopes and intercepts were calculated using ANCOVA). **k**) Food consumption (AL, n = 12; Diluted AL, n = 12; MF.cr, n = 12; CR, n = 11-12). All data are represented as mean ± SEM.

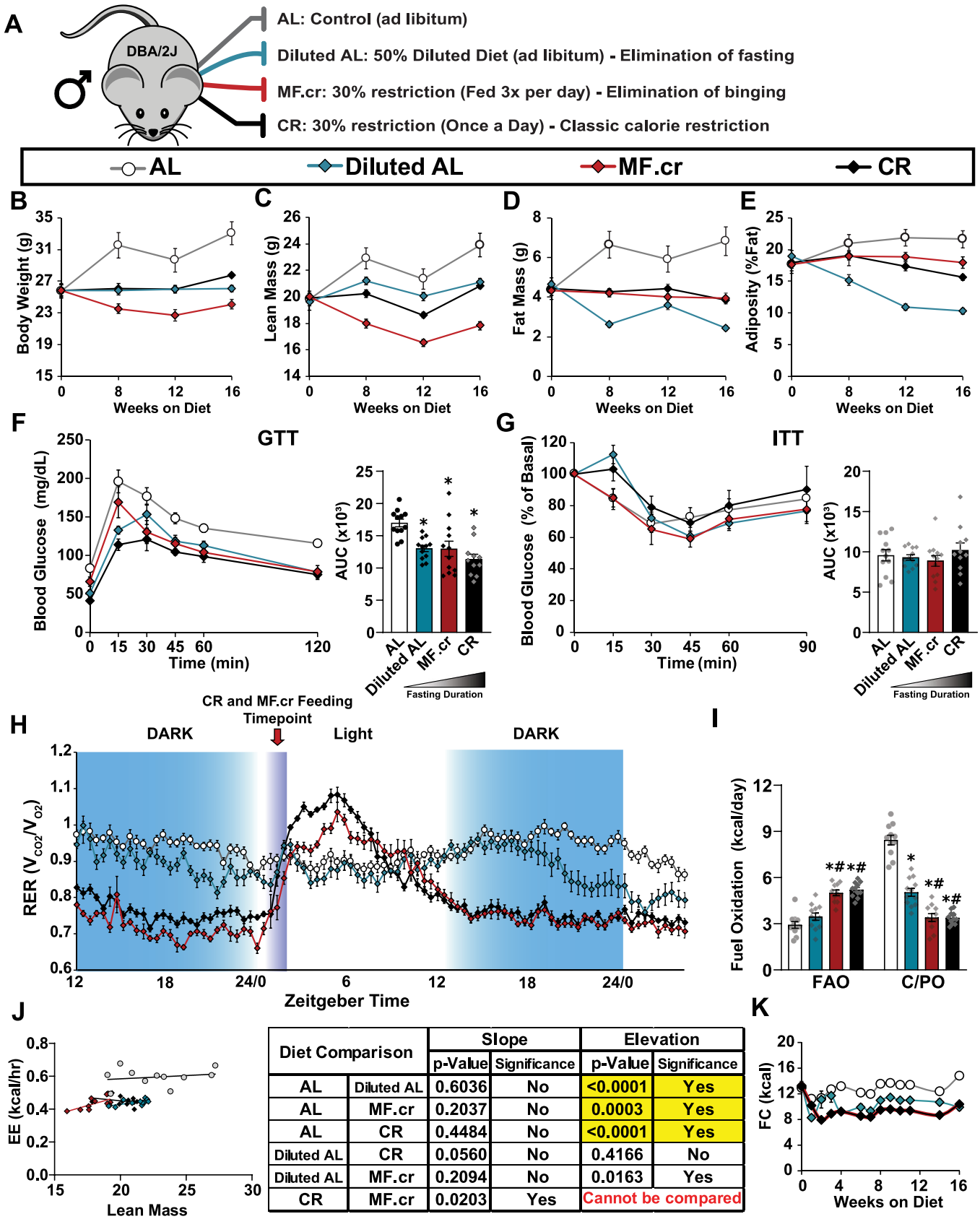

Diet Comparison		Slope		Elevation	
		p-Value	Significance	p-Value	Significance
AL	Diluted AL	0.6036	No	<0.0001	Yes
AL	MF.cr	0.2037	No	0.0003	Yes
AL	CR	0.4484	No	<0.0001	Yes
Diluted AL	CR	0.0560	No	0.4166	No
Diluted AL	MF.cr	0.2094	No	0.0163	Yes
CR	MF.cr	0.0203	Yes	Cannot be compared	

Extended Data Fig. 7 | See next page for caption.

Extended Data Fig. 7 | The effect of three calorie restriction regimens on male DBA/2J mice. (**a**) Outline of feeding regimens: AL, Diluted AL, CR and MF.cr. (**b–e**) Body composition measurement over 16 weeks on diet (AL, n = 11; Diluted AL, n = 11; MF.cr, n = 12; CR, n = 12 biologically independent mice); total body weight (**b**), lean mass (**c**), fat mass (**d**) and adiposity (**e**). (**f-g**) Glucose (AL, n = 12; Diluted AL, n = 12; MF.cr, n = 12; CR, n = 11 biologically independent mice) (**f**) and insulin (AL, n = 12; Diluted AL, n = 12; MF.cr, n = 12; CR, n = 11 biologically independent mice) (**g**) tolerance tests after 9 or 10 weeks on the indicated diets. * symbol represents a significant difference versus AL-fed mice (Diluted AL, $p = 0.0059$; MF.cr, $p = 0.0052$; CR, $p < 0.0001$) based on Tukey's test post one-way ANOVA. (H-J) Metabolic chamber analysis of mice fed the indicated diets. (**h**) Respiratory exchange ratio vs. time (AL, n = 12; Diluted AL, n = 11; MF.cr, n = 11; CR, n = 11 biologically independent mice) (**i**) Fuel utilization was calculated for the 24-hour period following the indicated (arrow) refeeding time (AL, n = 12; Diluted AL, n = 11; MF.cr, n = 11; CR, n = 11 biologically independent mice). * symbol represents a significant difference versus AL (Diluted AL, $p < 0.0001$; MF.cr, $p < 0.0001$; CR, $p < 0.0001$); # symbol represents a significant difference versus Diluted AL (MF.cr, $p \leq 0.0002$; CR, $p \leq 0.0001$) based on Tukey's test post one-way ANOVA performed separately for FAO and C/PO). (**j**) Energy expenditure as a function of lean mass was calculated for the 24-hour period following the indicated (arrow) refeeding time (AL, n = 12; Diluted AL, n = 11; MF.cr, n = 11; CR, n = 11 biologically independent mice, data for each individual mouse is plotted; slopes and intercepts were calculated using ANCOVA). K) Food consumption (n = 12 biologically independent mice per diet). All data are represented as mean ± SEM.

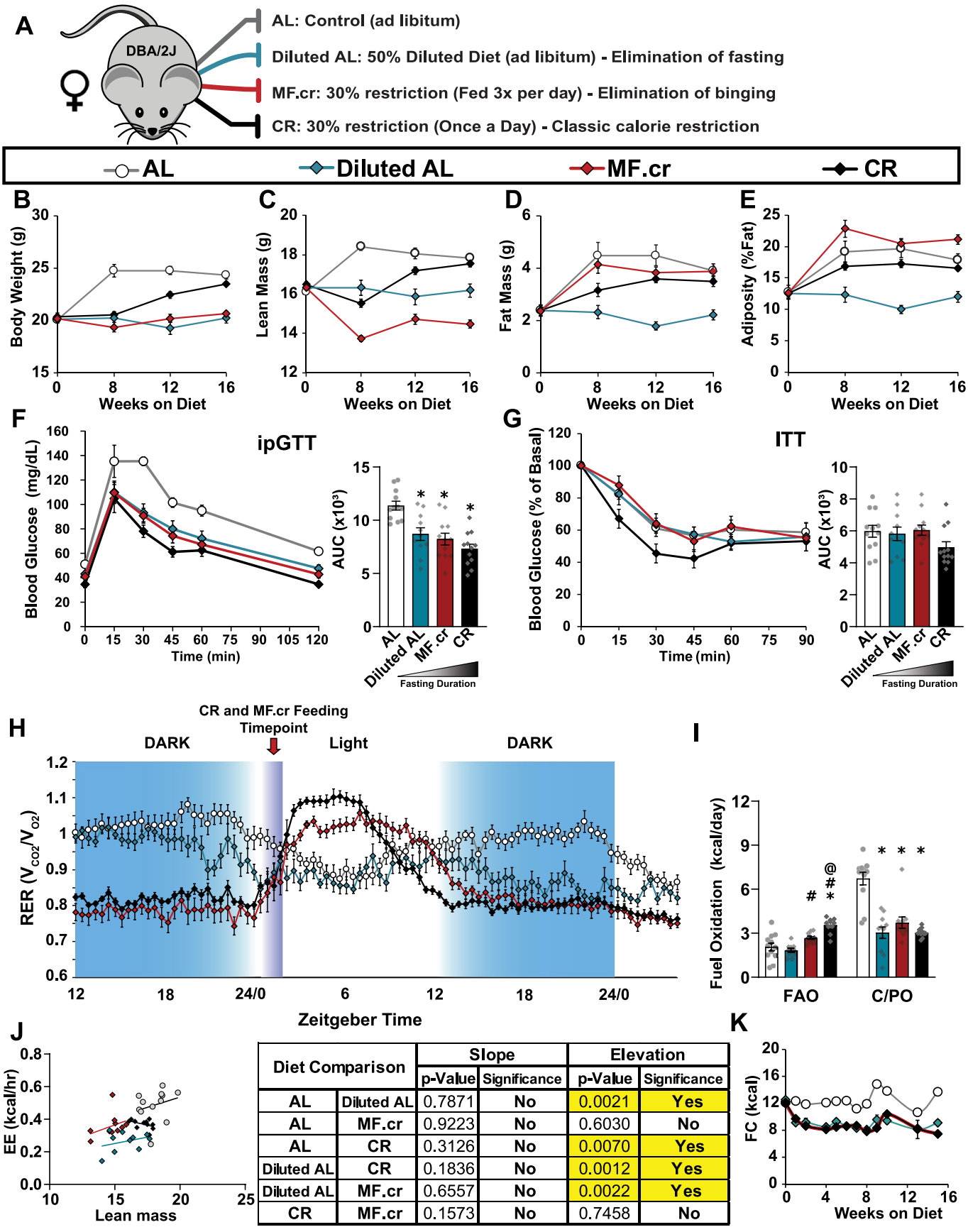

Diet Comparison		Slope		Elevation	
		p-Value	Significance	p-Value	Significance
AL	Diluted AL	0.7871	No	0.0021	Yes
AL	MF.cr	0.9223	No	0.6030	No
AL	CR	0.3126	No	0.0070	Yes
Diluted AL	CR	0.1836	No	0.0012	Yes
Diluted AL	MF.cr	0.6557	No	0.0022	Yes
CR	MF.cr	0.1573	No	0.7458	No

Extended Data Fig. 8 | See next page for caption.

Extended Data Fig. 8 | The effect of three calorie restriction regimens on female DBA/2J mice. (**a**) Outline of feeding regimens: AL, Diluted AL, CR and MF.cr. (**b-e**) Body composition measurement over 16 weeks on diet (AL, n = 12; Diluted AL, n = 7; MF.cr, n = 11; CR, n = 12 biologically independent mice); total body weight (**b**), lean mass (**c**), fat mass (**d**) and adiposity (**e**). (**f-g**) Glucose (AL, n = 12; Diluted AL, n = 11; MF.cr, n = 12; CR, n = 12 biologically independent mice) (**f**) and insulin (AL, n = 12; Diluted AL, n = 11; MF.cr, n = 12; CR, n = 12 biologically independent mice) (**g**) tolerance tests after 9 or 10 weeks on the indicated diets. * symbol represents a significant difference versus AL-fed mice (Diluted AL, $p = 0.0033$; MF.cr, $p = 0.0003$; CR, $p < 0.0001$) based on Tukey's test post one-way ANOVA. (H-J) Metabolic chamber analysis of mice fed the indicated diets. (**h**) Respiratory exchange ratio vs. time (AL, n = 11; Diluted AL, n = 11; MF.cr, n = 11; CR, n = 10 biologically independent mice) (**i**) Fuel utilization was calculated for the 24-hour period following the indicated (arrow) refeeding time (AL, n = 11; Diluted AL, n = 11; MF.cr, n = 11; CR, n = 10 biologically independent mice). * symbol represents a significant difference versus AL (Diluted AL, $p < 0.0001$; MF.cr, $p < 0.0001$; CR, $p < 0.0001$); # symbol represents a significant difference versus Diluted AL (MF.cr, $p \leq 0.0128$; CR, $p < 0.0001$); @ symbol represents a significant difference versus MF.cr (CR, $p \leq 0.0074$) based on Tukey's test post one-way ANOVA performed separately for FAO and C/PO). (J) Energy expenditure as a function of lean mass was calculated for the 24-hour period following the indicated (arrow) refeeding time (AL, n = 11; Diluted AL, n = 11; MF.cr, n = 11; CR, n = 10 biologically independent mice, data for each individual mouse is plotted; slopes and intercepts were calculated using ANCOVA). K) Food consumption (AL, n = 12; Diluted AL, n = 7-12; MF.cr, n = 12; CR, n = 12 biologically independent mice). All data are represented as mean ± SEM.

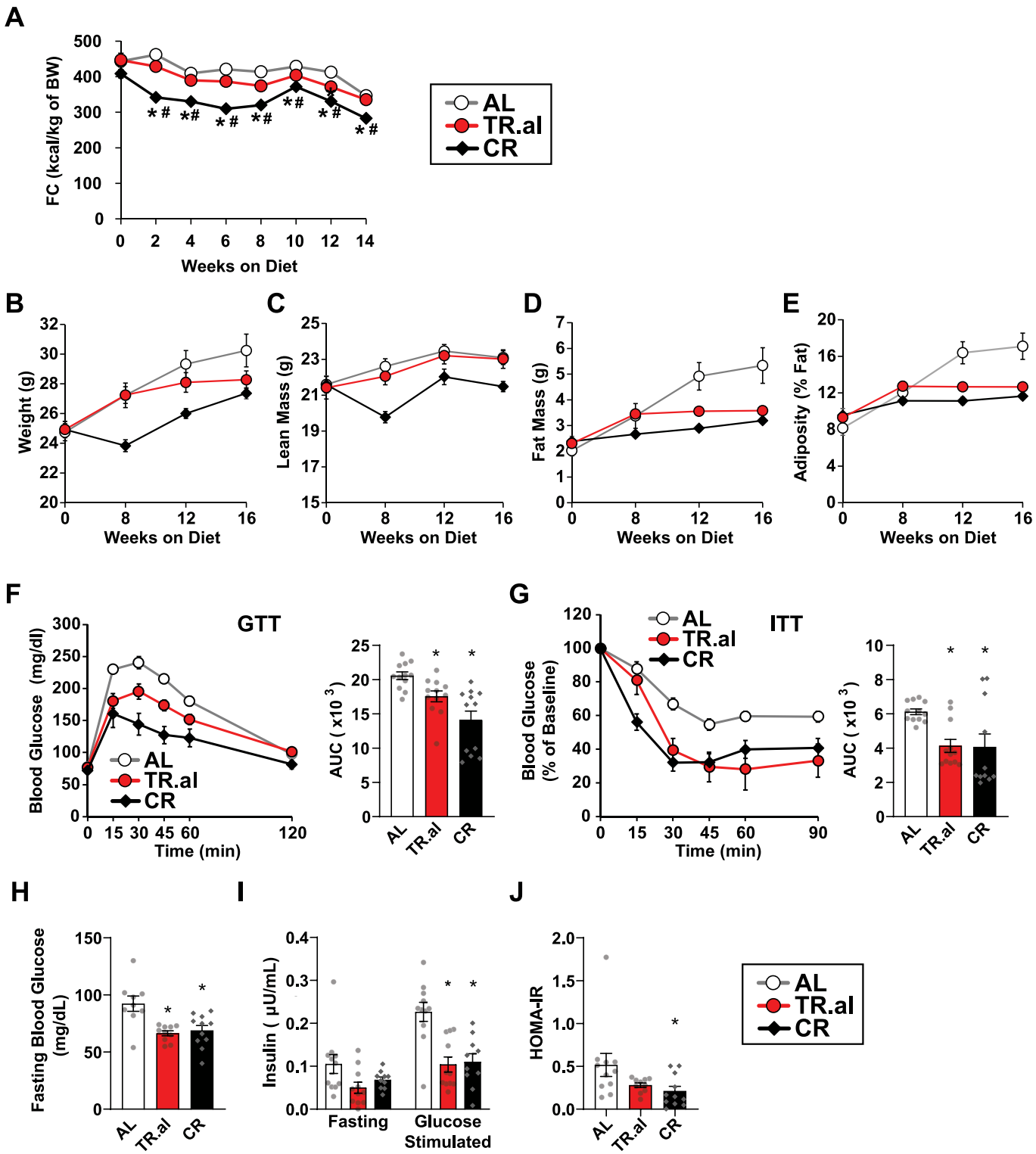

Extended Data Fig. 9 | Additional data for C57BL/6J male mice fed CR or TR.al diets. a) Food consumption (n = 12 biologically independent mice per diet). **b-e**) Body composition (body weight, lean mass, fat mass and adiposity) of C57BL/6J male mice fed the indicated diets for 4 months (n = 12 biologically independent mice per diet; statistics on supplementary table 7). F-G) Glucose (n = 12 biologically independent mice per diet) (**f**) and insulin (AL, n = 12; TR.al, n = 12; CR, n = 11 biologically independent mice) (**g**) tolerance tests were performed after 13-14 weeks, respectively on the indicated diets. (**h-j**) Fasting blood glucose (**h**), fasting and glucose-stimulated insulin secretion (15 minutes) (**i**), and calculated HOMA2-IR (**j**) (AL, n = 12; TR.al, n = 11; CR, n = 12 biologically independent mice). * symbol represents a significant difference versus AL (TR.al, $p \leq 0.0018$; CR, $p \leq 0.0477$); # symbol represents a significant difference versus TR.al (MF.cr, $p \leq 0.0187$; CR, $p = 0.0478$) based on Tukey's test post one-way ANOVA. All data are represented as mean ± SEM.

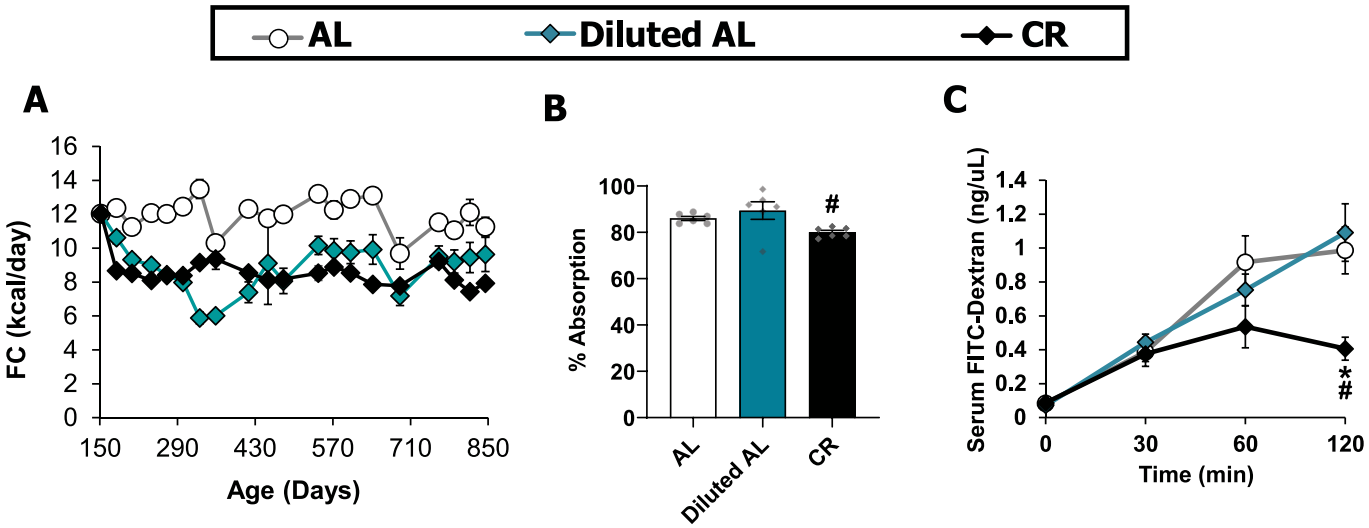

Extended Data Fig. 10 | Food consumption, absorption and gut integrity. a) Food consumption (AL, n = 27-33; Diluted AL, n = 8-33; CR, n = 30-33 biologically independent mice). **b**) Food absorption calculation by bomb calorimetry of 19-month-old C57BL/6J male mice fed the indicated diets for 13 months (n = 6 biologically independent mice per diet) **c**) Gut integrity calculation by FITC-dextran of 20-month-old C57BL/6J male mice (n = 6 biologically independent mice per diet). * symbol represents a significant difference versus AL (CR, $p = 0.0160$); # symbol represents a significant difference versus Diluted AL (CR, $p \leq 0.0281$) based on Tukey's test post two-way ANOVA) Data are represented as mean ± SEM.

nature research

Corresponding author(s): Lamming, Dudley

Last updated by author(s): Aug 25, 2021

Reporting Summary

Nature Research wishes to improve the reproducibility of the work that we publish. This form provides structure for consistency and transparency in reporting. For further information on Nature Research policies, see our Editorial Policies and the Editorial Policy Checklist.

Statistics

For all statistical analyses, confirm that the following items are present in the figure legend, table legend, main text, or Methods section.

n/a	Confirmed	
☐	☒	The exact sample size (*n*) for each experimental group/condition, given as a discrete number and unit of measurement
☐	☒	A statement on whether measurements were taken from distinct samples or whether the same sample was measured repeatedly
☐	☒	The statistical test(s) used AND whether they are one- or two-sided *Only common tests should be described solely by name; describe more complex techniques in the Methods section.*
☐	☒	A description of all covariates tested
☐	☒	A description of any assumptions or corrections, such as tests of normality and adjustment for multiple comparisons
☐	☒	A full description of the statistical parameters including central tendency (e.g. means) or other basic estimates (e.g. regression coefficient) AND variation (e.g. standard deviation) or associated estimates of uncertainty (e.g. confidence intervals)
☐	☒	For null hypothesis testing, the test statistic (e.g. *F*, *t*, *r*) with confidence intervals, effect sizes, degrees of freedom and *P* value noted *Give P values as exact values whenever suitable.*
☒	☐	For Bayesian analysis, information on the choice of priors and Markov chain Monte Carlo settings
☒	☐	For hierarchical and complex designs, identification of the appropriate level for tests and full reporting of outcomes
☒	☐	Estimates of effect sizes (e.g. Cohen's *d*, Pearson's *r*), indicating how they were calculated

Our web collection on statistics for biologists contains articles on many of the points above.

Software and code

Policy information about availability of computer code

Data collection	No software was used except for metabolic chambers (Oxymax v. 5.47 software from Columbus Instruments).
Data analysis	Data in this paper was analysed using Excel (2010 and 2016), Graphpad Prism 8, Spyder Anaconda 3, MAVEN 2011.6.17 and NetworkAnalyst Version 2

For manuscripts utilizing custom algorithms or software that are central to the research but not yet described in published literature, software must be made available to editors and reviewers. We strongly encourage code deposition in a community repository (e.g. GitHub). See the Nature Research guidelines for submitting code & software for further information.

Data

Policy information about availability of data

All manuscripts must include a data availability statement. This statement should provide the following information, where applicable:

- Accession codes, unique identifiers, or web links for publicly available datasets
- A list of figures that have associated raw data
- A description of any restrictions on data availability

The data that support the plots and other findings of this study are provided as a Source Data file or are available from the corresponding author upon reasonable request. RNA-sequencing data have been deposited with the Gene Expression Omnibus and are accessible through accession number GSE168262.

Field-specific reporting

Please select the one below that is the best fit for your research. If you are not sure, read the appropriate sections before making your selection.

☒ Life sciences ☐ Behavioural & social sciences ☐ Ecological, evolutionary & environmental sciences

For a reference copy of the document with all sections, see nature.com/documents/nr-reporting-summary-flat.pdf

Life sciences study design

All studies must disclose on these points even when the disclosure is negative.

Sample size	Sample sizes for longevity studies were determined in consultation with previously published power tables (Liang et al., 2003, Exp. Gerontol). Sample sizes for metabolic studies were determined based on our previously published experimental results with the effects of dietary interventions (Fontana and Cummings et al, 2016, Cell Reports), with the goal of having > 90% power to detect a change in area under the curve during a GTT ($p<0.05$). Data distribution was assumed to be normal, but this was not formally tested. Sample size for molecular analyses were not formally calculated, but chosen in consultation with core facility staff and experienced laboratory personnel.
Data exclusions	Data was not excluded.
Replication	The assays were chosen based on the evaluation of a number of criteria including good reproducibility, and are widely utilized by multiple groups. The effects of once-per-day CR in C57BL/6J male and female mice successfully reproduce results found in our previous studies as well as those from other laboratories. All data derived from animal experiments represent the results obtained from at least three biologically independent animals. There were no attempts at replication of specific results in young animals, but animals were assessed for many phenotypes at multiple time points, and results at later time points reproduced those at earlier time points as included in the manuscript. Metabolic results in the longevity study reproduced the results in C57BL/6J young mice. Molecular profiling experiments were performed once; pathways and metabolite changes detected for once per day CR replicate those in previous studies as discussed in the manuscript text.
Randomization	All studies were performed on animals or tissues collected from animals. Animals of each sex and strain were randomized into groups of equivalent weight prior to the beginning of the in vivo studies.
Blinding	Investigators were blinded to diet groups during data collection whenever feasible, but this was not usually possible or feasible as as cages were clearly marked to indicate the diet provided, and the size and body composition of the mice was altered by strain and diet. However, blinding is not relevant to the majority of the studies conducted here, as the data is collected in numeric form which is not readily subject to bias due to the need for subjective interpretation. Investigators were not blinded during necropsies, as the size and body composition of the mice was altered by strain and diet and group identity was therefore readily apparent.

Reporting for specific materials, systems and methods

We require information from authors about some types of materials, experimental systems and methods used in many studies. Here, indicate whether each material, system or method listed is relevant to your study. If you are not sure if a list item applies to your research, read the appropriate section before selecting a response.

Materials & experimental systems

n/a	Involved in the study
☒	☐ Antibodies
☒	☐ Eukaryotic cell lines
☒	☐ Palaeontology and archaeology
☐	☒ Animals and other organisms
☒	☐ Human research participants
☒	☐ Clinical data
☒	☐ Dual use research of concern

Methods

n/a	Involved in the study
☒	☐ ChIP-seq
☒	☐ Flow cytometry
☒	☐ MRI-based neuroimaging

Animals and other organisms

Policy information about studies involving animals; ARRIVE guidelines recommended for reporting animal research

Laboratory animals	C57BL/6J male mice at ages ranging from 2 months of age to approximately 3 years of age were used. C57BL/6J female mice, DBA/2J male mice, and DBA/2J female mice at ages ranging from 8 weeks to 6 months of age were used. All mice were obtained from The Jackson Laboratory.
Wild animals	No wild animals were used in the study.
Field-collected samples	No field collected samples were used in the study.

Ethics oversight	Animal studies were approved by the Institutional Animal Care and Use Committee of the William S. Middleton Memorial Veterans Hospital (Assurance ID: D16-00403), Madison, WI.

Note that full information on the approval of the study protocol must also be provided in the manuscript.